



National Library
of Canada

Acquisitions and
Bibliographic Services Branch

395 Wellington Street
Ottawa, Ontario
K1A 0N4

Bibliothèque nationale
du Canada

Direction des acquisitions et
des services bibliographiques

395, rue Wellington
Ottawa (Ontario)
K1A 0N4

Your file *Votre référence*

Our file *Notre référence*

NOTICE

The quality of this microform is heavily dependent upon the quality of the original thesis submitted for microfilming. Every effort has been made to ensure the highest quality of reproduction possible.

If pages are missing, contact the university which granted the degree.

Some pages may have indistinct print especially if the original pages were typed with a poor typewriter ribbon or if the university sent us an inferior photocopy.

Reproduction in full or in part of this microform is governed by the Canadian Copyright Act, R.S.C. 1970, c. C-30, and subsequent amendments.

AVIS

La qualité de cette microforme dépend grandement de la qualité de la thèse soumise au microfilmage. Nous avons tout fait pour assurer une qualité supérieure de reproduction.

S'il manque des pages, veuillez communiquer avec l'université qui a conféré le grade.

La qualité d'impression de certaines pages peut laisser à désirer, surtout si les pages originales ont été dactylographiées à l'aide d'un ruban usé ou si l'université nous a fait parvenir une photocopie de qualité inférieure.

La reproduction, même partielle, de cette microforme est soumise à la Loi canadienne sur le droit d'auteur, SRC 1970, c. C-30, et ses amendements subséquents.

Canada

IONIC, METABOLIC AND CONTRACTILE FUNCTION CHANGES IN THE
ISOLATED RAT HEART DURING ISCHEMIA AND REPERFUSION:
 ^7Li , ^{23}Na AND ^{31}P NMR SPECTROSCOPY STUDIES

Claudia Anne Keon

Department of Physiology

University of Ottawa

and

Institute for Biodiagnostics

National Research Council

A thesis submitted for the
Master of Science Degree in Physiology, within
the University of Ottawa.

July, 1992.



Claudia Anne Keon, Ottawa, Canada, 1992



National Library
of Canada

Bibliothèque nationale
du Canada

Acquisitions and
Bibliographic Services Branch

Direction des acquisitions et
des services bibliographiques

395 Wellington Street
Ottawa, Ontario
K1A 0N4

395, rue Wellington
Ottawa (Ontario)
K1A 0N4

Your file *Votre référence*

Our file *Notre référence*

The author has granted an irrevocable non-exclusive licence allowing the National Library of Canada to reproduce, loan, distribute or sell copies of his/her thesis by any means and in any form or format, making this thesis available to interested persons.

L'auteur a accordé une licence irrévocable et non exclusive permettant à la Bibliothèque nationale du Canada de reproduire, prêter, distribuer ou vendre des copies de sa thèse de quelque manière et sous quelque forme que ce soit pour mettre des exemplaires de cette thèse à la disposition des personnes intéressées.

The author retains ownership of the copyright in his/her thesis. Neither the thesis nor substantial extracts from it may be printed or otherwise reproduced without his/her permission.

L'auteur conserve la propriété du droit d'auteur qui protège sa thèse. Ni la thèse ni des extraits substantiels de celle-ci ne doivent être imprimés ou autrement reproduits sans son autorisation.

ISBN 0-315-85802-8

Canada



UNIVERSITÉ D'OTTAWA
UNIVERSITY OF OTTAWA

ACKNOWLEDGEMENTS

This work was carried out in the Institute for Biodiagnostics of the National Research Council of Canada in conjunction with the Department of Physiology of the University of Ottawa.

I would like to express my sincere gratitude and appreciation to my supervisor, Dr. Kieran Clarke for her expert advice and patient guidance over the last two years. Many thanks are also extended to Dr. Jean-François Nédélec who worked with me on this project and who provided a great deal of valuable instruction in NMR techniques. I would also like to thank Dr. Roxanne Deslauriers, Dr. John Saunders and Dr. Ian Smith for their input and encouragement during the period of this study.

I would also like to thank Elizabeth Rokosh, Victor Boyko and Jim McLaren for their time and effort in assisting me with the ICP-AES and bench experiments in this study.

Finally, I would like to thank my parents, Anne and Wilbert Keon, for their unflagging support and encouragement.

STATEMENT

The work reported in this thesis was undertaken in the Institute for Biodiagnostics of the National Research Council of Canada in conjunction with the Department of Physiology of the University of Ottawa, under the supervision of Dr. Kieran Clarke.

I declare that the work presented in this thesis is, to the best of my knowledge and belief, original except as acknowledged in the text; and that this material has not previously been submitted, either in part or in full, for a degree at this or any other university.

Claudia Anne Keon

July, 1992

ABSTRACT

^7Li NMR spectroscopy has been used to investigate the transsarcolemmal transport mechanisms responsible for the increase in intracellular sodium that occurs during global ischemia in the isolated rat heart. Hearts were perfused with a modified Krebs Henseleit buffer containing 78 mM sodium and 78 mM lithium, lithium being a biological congener for sodium with twice the sodium NMR sensitivity. In order to accurately quantify ^7Li NMR signals, the NMR relaxation times for lithium were investigated in the perfused heart and buffer solutions. The T_1 for lithium in Krebs Henseleit buffer was 24 s and the T_2 was 19 s, whereas in the perfused heart, total lithium had a T_1 of 7 s and a biexponential T_2 with a fast component of 0.17 s and a slow component of 0.85 s. The addition of the shift reagent, DyTTHA^{3-} , shortened the relaxation times for lithium in buffer and enabled the discrimination of intra- and extracellular lithium. Intracellular lithium had a T_1 of ~9 s, which was unaffected by the presence of shift reagent in the extracellular space and it had a biexponential T_2 with a fast component of 0.04 s and a slow component of 1.12 s. Perfusion of the hearts with shift reagent enabled us to characterise the kinetics of lithium movement across the sarcolemma. Lithium moved into the myocardial cells with a rate constant (k_1) of 0.068 min^{-1} , a $t_{1/2}$ of 10.3 min and an initial rate of increase of 5.27 mM/min , while lithium moved out of the heart with a k_1 of 0.062 min^{-1} , a $t_{1/2}$ of 11.2 min and an initial rate of 4.83 mM/min . Lithium equilibrated in the heart with equal concentrations on either side of the sarcolemma, not in equilibrium with its electrochemical gradient. Perfusion with the low-sodium, lithium-containing buffer had a positive inotropic effect on the heart with no effect on the steady state levels of the myocardial high energy phosphates. The myocardial rate pressure product increased by 114% while the ATP and PCr concentrations, measured using ^{31}P NMR spectroscopy, varied by less than 8%. We showed that the increase in cardiac contractility was not due to a direct effect of lithium on the myocardium, but rather to the decrease in the transsarcolemmal sodium gradient which caused a decrease in $\text{Na}^+/\text{Ca}^{2+}$

exchange and resulted in an overall increase in $[Ca^{2+}]_i$. ICP-AES analysis of hearts showed that as lithium accumulated in the cells, it displaced both sodium and potassium. We used ^{23}Na and 7Li NMR spectroscopy to examine the uptake of sodium and lithium during sodium pump inhibition and found that lithium accumulation in the heart was 43% greater than sodium accumulation. Finally, intracellular lithium increased during myocardial ischemia with a linear rate of 1.34 mM/min, similar to the rate of increase of intracellular sodium during ischemia. This increase was completely blocked by the Na^+/H^+ exchange inhibitor, amiloride. Thus, it can be concluded that Na^+/H^+ exchange is most likely the major mechanism for the increase in $[Na^+]_i$ during ischemia.

TABLE OF CONTENTS

	Page
Acknowledgements	i
Statement	ii
Abstract	iii-iv
Table of Contents	v-vii
List of Figures	viii-ix
List of Tables	x
Chapter 1	General Introduction
1.1	Central Role of Sodium in Cardiac Physiology 2
1.2	^{23}Na NMR Spectroscopy and Shift Reagents 6
1.3	Lithium as a Biological Congener for Sodium 8
1.4	^7Li NMR Spectroscopy 9
Chapter 2	General Methods
2.1	Perfused hearts 11
2.2	Shift reagents 12
2.3	Perfusion buffers 12
2.4	Bathing solutions 13
2.5	Washout Solutions 14
2.6	External Standards 14
2.7	NMR Spectroscopy 15
2.8	Inductively Coupled Plasma Atomic Emission Spectroscopy 15
2.9	Statistical Analysis 16

Chapter 3	Lithium Relaxation Parameters	
3.1	Introduction	18
3.2	Methods	
3.2.1	Determination of Relaxation Parameters	19
3.2.2	Experimental Protocol	20
3.2.3	Data Analysis	22
3.3	Results	22
3.4	Discussion	26
Chapter 4	Lithium Wash-in and Washout Kinetics and Lithium Uptake During Ischemia	
4.1	Introduction	31
4.2	Methods	
4.2.1a	Wash-in and Ischemia Protocols	31
4.2.1b	Data Analysis	32
4.2.2a	Washout Protocol	33
4.2.2b	Data analysis	33
4.3	Results	
4.3.1	Wash-in	34
4.3.2	Ischemia	35
4.3.3	Washout	36
4.4	Discussion	38
Chapter 5	Cardiac Function and Energetics During Lithium Perfusion	
5.1	Introduction	46
5.2	³¹ P NMR Spectroscopy	
5.2.1	Lithium Perfusion	47

5.2.2	Ischemia and Reperfusion	47
5.3	Bench Experiments	48
5.4	Results	48
5.5	Discussion	55
Chapter 6	Characterisation of Transsarcolemmal Lithium Transport Mechanisms	
6.1	Introduction	60 a
6.2	Methods	
6.2.1	Amiloride and Li^+/H^+ exchange	61
6.2.2	Ouabain and Na^+ Pump Activity	62
6.3	Results	
6.3.1	Amiloride and Li^+/H^+ exchange	63
6.3.2	Ouabain and Na^+ Pump Activity	64
6.4	Discussion	68
Chapter 7	General Conclusions	72
References		74
Publications		82

LIST OF FIGURES

<u>Figure</u>	<u>Page</u>
1.1 Schematic of the sarcolemma illustrating the various ion transport mechanisms	5
1.2 Structure of the DyTTTHA ³⁻ molecule	7
3.1 Lithium spectra from the isolated perfused rat heart, with and without shift reagent	23
4.1 Lithium uptake by the myocardium during perfusion with Krebs Henseleit buffer containing 78 mM lithium	34
4.2 Lithium uptake during myocardial ischemia	35
4.3 Washout of lithium from the myocardium	36
5.1 ³¹ P NMR spectrum from an isolated, perfused rat heart	46
5.2 Representative pressure and heart rate tracing from an isolated heart perfused with KH and LKH buffers	49
5.3 Change in PCr during pre-ischemia, ischemia and reperfusion, with and without lithium	52
5.4 Change in ATP during pre-ischemia, ischemia and reperfusion, with and without lithium	53
5.5 Change in Pi during pre-ischemia, ischemia and reperfusion, with and without lithium	54
5.6 Change in pH during pre-ischemia, ischemia and reperfusion, with and without lithium	55
5.7 Computer modelling of the effects of low sodium perfusion on the SA nodal and ventricular cells of the heart	57
6.1 ²³ Na NMR spectra from the rat heart perfused with LKHS containing ouabain and zero potassium	65

6.2 ^7Li NMR spectra from the rat heart perfused with LKHS containing ouabain and zero potassium	66
---	----

LIST OF TABLES

<u>Table</u>	<u>Page</u>
1.1 NMR properties of selected alkali metal nuclei	6
2.1 Composition of perfusion buffers (mM)	13
3.1 Perfusion conditions used for the measurement of lithium relaxation times in heart	21
3.2 Lithium T ₁ values in perfusion buffer and the perfused rat heart	24
3.3 Lithium T ₂ values in perfusion buffer and the perfused rat heart	25
3.4 Lithium T ₁ /T ₂ values in perfusion buffer and the perfused rat heart	28
4.1 Intracellular lithium concentrations during wash-in and ischemia	37
4.2 Intracellular cation concentrations in control and lithium perfused hearts determined by ICP-AES	37
4.3 Free energy changes for electrically neutral ion exchanges during lithium wash-in	41
4.4 Free energy changes for electrically neutral ion exchanges during lithium wash-out	42
5.1 Effect of LKH perfusion on myocardial function and flow	50
5.2 Statistical results of a split plot analysis of variance and covariance with repeated measures on steady state levels of PCr, ATP, Pi and pH of LKH perfused hearts	52
6.1 Effect of 1 mM amiloride on lithium uptake during perfusion and ischemia	63
6.2 Intracellular lithium and sodium concentrations after 20 min perfusion with LKH containing ouabain and zero potassium	67
6.3 Intracellular cation concentrations after 20 min perfusion with various buffers, measured using ICP-AES	68

CHAPTER ONE

GENERAL INTRODUCTION

1.1 Central Role of Sodium in Cardiac Physiology

1.2 ^{23}Na NMR Spectroscopy and Shift Reagents

1.3 Lithium as a Biological Congener for Sodium

1.4 ^7Li NMR Spectroscopy

1.1 Central Role of Sodium in Cardiac Physiology

Sodium, a key cation involved in the maintenance and function of myocardial cells, is present in the extracellular spaces at a concentration of 144 mM and has an intracellular concentration between 5 and 20 mM. The sodium ion carries a positive charge which results in an electrical force on the extracellular cation from the negatively charged intracellular space. The equilibrium potential for sodium is +49 millivolts while the actual resting membrane potential (E_m) is -85 millivolts. This large concentration gradient and electrical potential result in an inward driving force on sodium. The potential energy of this force is harnessed to drive several transmembrane ionic exchange processes, such as Na^+/H^+ , $\text{Na}^+/\text{Ca}^{++}$ and $\text{Na}^+/\text{K}^+/\text{Cl}^-$ exchanges (Fig.1.1). The gradient is maintained by the relative impermeability of the sarcolemma to the sodium ion and by the continuous extrusion of sodium by the electrogenic Na^+/K^+ -ATPase (Na^+ pump), which pumps sodium out of the intracellular space and pumps in potassium in the ratio of 3 Na^+ :2 K^+ . It has been postulated that a large amount of the total intracellular potassium present in myocardial cells is either bound or sequestered and thus is not free to contribute to the resting membrane potential, consequently it may be more appropriate to use the intracellular activity of potassium which estimates the concentration of the free ionized cation (Opie, 1991). Unsequestered potassium is present in heart cells at a concentration (estimated by the intracellular activity) of ~80 mM (Dalby *et. al.*, 1981; Lee and Fozzard, 1975) and it has an extracellular concentration of 4.7 mM resulting in an equilibrium potential of -76 millivolts which is much closer to the resting membrane potential than the sodium equilibrium potential. As a consequence, the resting membrane potential is determined mostly by the free potassium ion concentration gradient across the sarcolemma. The electrogenic sodium pump generates another -10 mV, which when added to the potassium equilibrium potential gives a value of -86 mV, very close to the measured potential of -85 mV (Opie, 1991).

Sodium is able to exchange for protons in the electrically neutral Na^+/H^+ antiporter. This exchanger plays a major role in the maintenance of intracellular pH, mainly during ischemia when its activity is maximised by intracellular acidosis (Lazdunski *et al.*, 1985; Aronson, 1985). However, Lazdunski *et al.* (1985) have also postulated that the activity of this exchanger would most likely be reduced during global ischemia because the drop in extracellular pH would offset the stimulatory effects of the intracellular acid load.

Sodium in exchange for calcium is involved in the regulation of $[\text{Ca}^{2+}]_i$ during excitation-contraction coupling (Powell and Noble, 1989). This exchanger is electrogenic, exchanging 3 Na^+ for 1 Ca^{2+} its activity depending on the concentrations of the ions involved and on the membrane potential (Kimura *et al.*, 1986). The exchanger is very sensitive to intracellular calcium concentrations, providing a major route for calcium efflux when the cell is at the resting membrane potential. In this case, sodium moves into the cell, down its electrochemical gradient and calcium is moved out against its electrochemical gradient. This exchanger can reverse its direction when the membrane is depolarised to around -40 mV (Ravens and Wettwer, 1989), for example at the peak of the action potential and during ischemia when the membrane becomes depolarised. In fact, reversed $\text{Na}^+/\text{Ca}^{2+}$ exchange may be favored during ischemia because the exchanger is sensitive to increases in intracellular sodium causing the potential at which the exchanger reverses to become less negative (Ravens and Wettwer, 1989).

During myocardial ischemia, there is no flow of blood (or buffer solution) to the heart, metabolic waste products accumulate and the ionic content of the cells changes. Creatine phosphate breaks down rapidly to produce creatine and inorganic phosphate. ATP breaks down at slower rate to produce ADP, adenosine, inorganic phosphate and protons. Glycogen stores are consumed and lactate and protons are produced as the cells rapidly switch from aerobic to anaerobic metabolism (Neely and Grotyohann, 1984). These events lead to a severe drop in intracellular pH and a build-up of P_i , lactate and ADP, all of which may inhibit the

activity of the Na^+ pump (Tani and Neely, 1989). This, in turn, leads to a significant rise in intracellular sodium concentration, a decrease in intracellular potassium and depolarization of the resting membrane potential (Opie, 1991). A rise in intracellular sodium occurs rapidly with the onset of ischemia (Murphy et al, 1991). The hearts stop beating quickly after the flow is turned off, with closing of the fast sodium channels (Poole-Wilson, 1984), therefore an influx mechanism must exist which would contribute to the rise in intracellular sodium during ischemia. A prime suspect for this mechanism is Na^+/H^+ exchange which is, as previously stated, maximally activated by an intracellular acid load and which uses the transsarcolemmal sodium gradient to transport protons out of the cell.

Upon reperfusion, the extracellular pH and sodium rapidly return to control levels and Na^+/H^+ exchange is stimulated. The re-establishment of the sodium gradient across the sarcolemma may occur by several mechanisms including the restoration of the sodium pump activity, $\text{Na}^+/\text{H}_2\text{PO}_4^-$ cotransport, sodium dependent bicarbonate exchange and reversed $\text{Na}^+/\text{Ca}^{2+}$ exchange. The latter may cause a rise in $[\text{Ca}^{2+}]_i$ which could trigger the release of more Ca^{2+} from intracellular sarcoplasmic reticular stores. A massive increase in $[\text{Ca}^{2+}]_i$ during reperfusion has been associated with a permanent degeneration of myocardial contractile function accompanied by calcium phosphate precipitation in mitochondria (Lehninger, 1974).

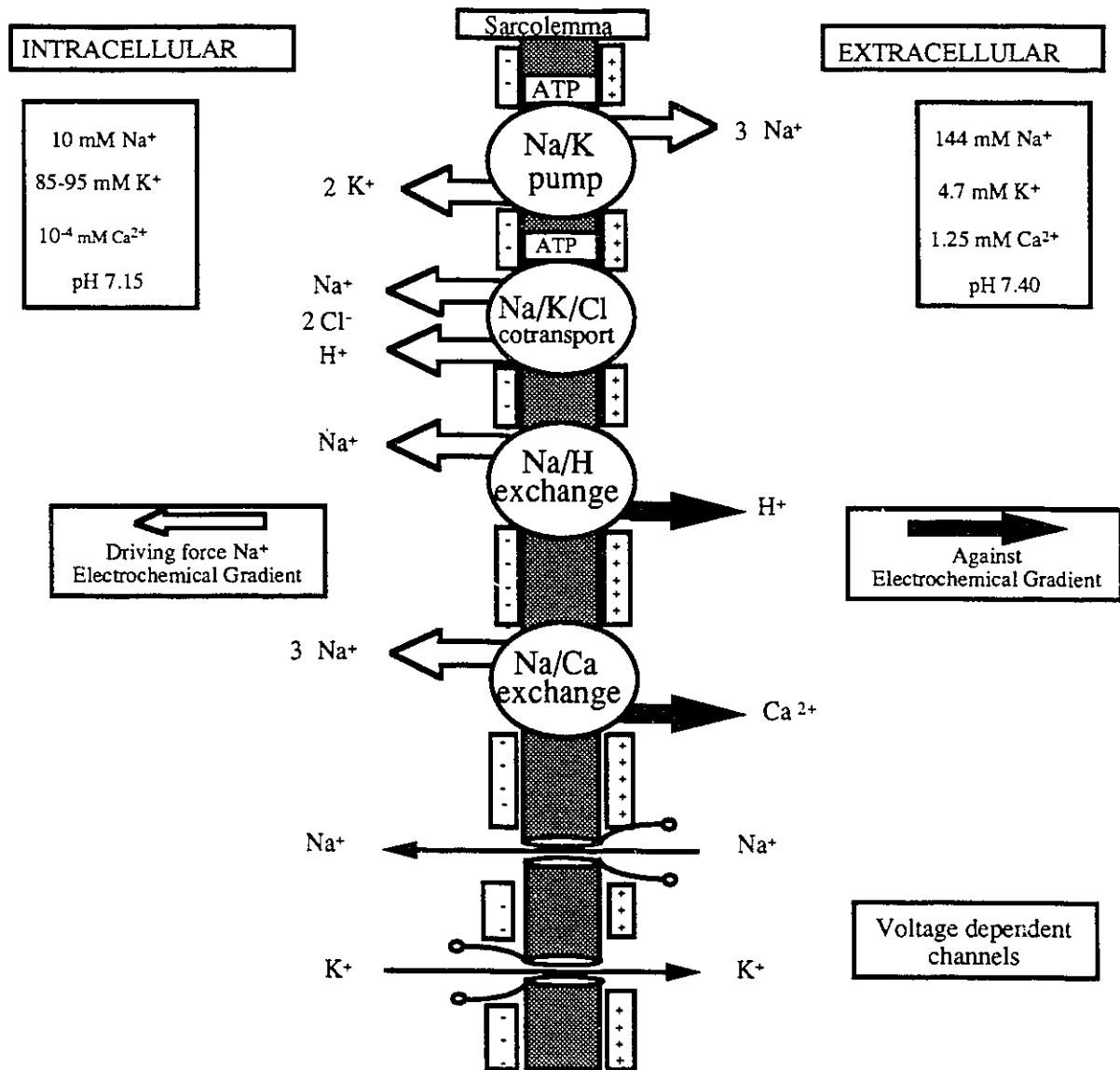


Fig. 1.1 Schematic illustrating some of the important sodium transport mechanisms.

1.2 ^{23}Na NMR Spectroscopy and Shift Reagents

^{23}Na NMR spectroscopy can be used to noninvasively study myocardial sodium. The sodium nuclide that possesses a magnetic moment is 100% abundant and has an effective NMR sensitivity of 50 (Table 1). This combination of factors makes the sodium nucleus very attractive for NMR studies. Unfortunately, sodium exists mainly as an aqueous cation in both the intra- and extracellular compartments, so the ^{23}Na NMR signals from each compartment are isochronous, appearing as a single peak in the spectrum. In order to study the transsarcolemmal sodium gradient, it is necessary to employ shift reagents (SR) to distinguish between intra- and extracellular Na^+ signals (Pike, 1985).

Table 1: NMR Properties of Selected Alkali Metal Nuclei

Nucleus	Natural abundance (%)	Gyromagnetic ratio ($\text{g}/10^7 \text{ rad T}^{-1}\text{s}^{-1}$)	Effective sensitivity*
^7Li	93	10.4	101
^{23}Na	100	7.08	50

*Calculated by natural abundance x gyromagnetic ratio² for the same number of nuclei at constant field

Shift reagents are anionic chelate complexes of molecules similar to ethylenediaminetetraacetic acid (EDTA) and paramagnetic lanthanides such as Dy^{3+} (Fig.1.2) or Tm^{3+} . The anionic nature of the SR allows it to form rapidly an ion-pair equilibrium with the cationic nuclei to be observed. Due to the rapid and transient nature of the cation binding to the SR, the observed NMR signal is the average of that of the free ion and the bound ion and

the resultant signal is shifted away from the zero position in the spectrum that corresponds to the unshifted Na^+ signal. The anionic nature of the SR also ensures that binding to negatively charged macromolecules and membrane surfaces is minimized. The charge and size of the SR molecules render them unable to cross cell membranes. The SR, DyTTHA^{3-} (TTHA^{6-} : triethylenetetraminehexaacetate) has been used in our studies because the paramagnetic lanthanide Dy^{3+} never leaves the TTHA^{6-} chelation cage, ensuring that this shift reagent is not toxic to the myocardium (Springer, 1987). DyTTHA^{3-} moves into the extracellular spaces of the perfused heart within approximately two minutes where it interacts with cations to cause a shift in their resonances and enables the discrimination of intra- and extracellular cations.

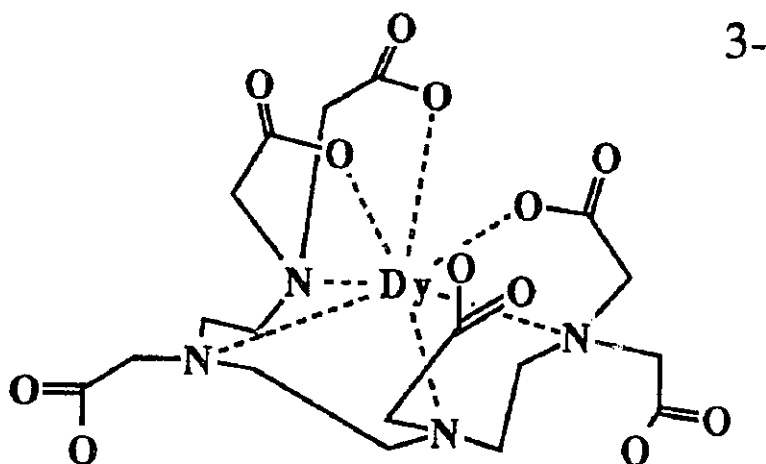


Fig. 1.2 Structure of the DyTTHA^{3-} molecule.

The intensity of the spectral peak is proportional to the amount of the ion and depends on the product of the ion concentration and volume of the compartment. The extracellular spaces of the heart contain about 99% of the Na^+ , the other 1% being intracellular. Consequently the ^{23}Na NMR spectrum consists of a large shifted extracellular Na^+ signal and a very small unshifted intracellular Na^+ signal, which is often difficult to quantify (Kohler *et al.*,

1991). These quantification difficulties have led to our use of lithium as a probe for sodium movements across the myocardial cell membrane.

1.3 Lithium as a Biological Congener for Sodium

Lithium is a biological congener for sodium. It is a small alkali earth metal cation that is able to replace sodium in many transmembrane exchange processes (Fig.1). In 1964, Carmeliet was able to demonstrate that lithium was capable of replacing sodium in the mechanism generating the cardiac action potential, indicating that lithium is able to pass through fast sodium channels. Carmeliet (1964) also demonstrated that the resting membrane permeability to lithium is high and that lithium accumulates in the cell and is not actively pumped out, indicating that the Na^+ pump has a very low affinity for lithium. The $\text{Na}^+/\text{Ca}^{2+}$ antiporter likewise seems to be unable to accept lithium as a substitute for sodium (Ponce-Hornos and Langer, 1980). Lithium can cross the cell membrane in exchange for protons, as demonstrated in studies on the Na^+/H^+ exchanger in red blood cells, in cardiac myocytes and in nerve cells (Mahnensmith and Aronson, 1985). Lithium may be able to substitute for sodium in the $\text{Na}^+/\text{K}^+/\text{Cl}^-$ cotransporter, but there is currently no information available on the affinity of this transporter for lithium.

The lithium cation exhibits a high degree of hydration. It has a small radius and positive charge which enables many water molecules to pack tightly around it. The potassium ion shows a much lower degree of hydration and the water molecules are easily stripped off (Stein, 1990). This has been postulated to contribute to the specificity of the voltage regulated potassium channel. It is thought that the potassium ions pass through the channel in single file, displacing their water molecules as they form transient bonds with weakly anionic residues lining the inside of the channel. The high degree of hydration and the relatively greater strength

of the hydration bonding to the lithium ion would inhibit its passage through the channel in a similar manner (Stein, 1990).

The working hypothesis for our studies is that the Na^+/H^+ antiporter is the principal mechanism by which sodium is transported into the cell during ischemia, with sodium pump inhibition by products of anaerobic glycolysis preventing efflux. Lithium has been shown to replace sodium in Na^+/H^+ exchange and the contribution from the $\text{Na}^+/\text{Ca}^{2+}$ exchanger can be ignored since lithium cannot substitute for sodium in this exchanger. The ability of lithium to replace sodium in the fast sodium channel and the Na^+/H^+ exchanger, as well as its high NMR sensitivity and natural abundance (Table 1), combine to make lithium a very attractive probe to study sodium transport mechanisms during ischemia.

1.4 ^7Li NMR Spectroscopy

The $^7\text{Li}^+$ nuclide is 93% abundant and its effective NMR sensitivity (gyromagnetic ratio² x natural abundance) is 101, which is twice that of $^{23}\text{Na}^+$ (Table 1). Unlike sodium, this nucleus is only weakly quadrupolar in nature and therefore has a much longer longitudinal relaxation time in solution (Woessner, 1989). There are no published values for the relaxation times of intracellular lithium in heart under physiological conditions. As a consequence, these were the first parameters to be investigated in our studies. Once the relaxation characteristics of lithium had been established, we were able to conduct kinetic experiments in which the influx and efflux rates for lithium crossing the sarcolemma were determined. In our experiments, the entire source of lithium was exogenous, so there were no complications arising from intracellular stores of lithium. The rate of lithium uptake during ischemia was established and specific sodium exchange inhibitors were used to characterize the mechanisms of lithium uptake during ischemia.

CHAPTER TWO
GENERAL METHODS

- 2.1 Perfused Hearts
- 2.2 Shift Reagents
- 2.3 Perfusion Buffers
- 2.4 Bathing Solutions
- 2.5 Washout Solutions
- 2.6 External Standards
- 2.7 NMR Spectroscopy
- 2.8 Inductively Coupled Plasma Atomic
Emission Spectroscopy (ICP-AES)
- 2.9 Data Analysis

2.1 Perfused Hearts

Male, Sprague-Dawley rats weighing 350-450g were anesthetized by intraperitoneal injection of 6.5 mg/100 g body weight of sodium pentobarbital. The hearts were rapidly excised (< 30 s) and submerged in ice-cold phosphate-free Krebs Henseleit buffer (KH; Table 2.1) that was gassed with 95% O₂: 5% CO₂ to give a pH of 7.40. The immersion of the heart in cooled perfusion buffer causes it to arrest which protects it during mounting on the cannula. Hearts were cannulated by the ascending aorta in a standard Langendorff preparation and perfused at a constant pressure of 100 mmHg, a pressure that is equivalent to the average diastolic blood pressure of the rat heart in vivo (Baker, 1980). Retrograde perfusion closes the aortic valve and delivers the perfusate into the coronary arteries from which it then passes out into the coronary sinus and right atrium (Doring, 1988). A length of polyethylene tubing was inserted through a slit in the left atrial appendage and guided through the left ventricular wall at the apex of the heart to provide a drain. A latex balloon connected to a Gould 2200S pressure transducer and recorder, was then inserted into the left ventricle and inflated with water until an end diastolic pressure of 5-10 mmHg was attained. The balloon had a volume that was slightly greater than the volume of the ventricle (to minimise ventricular fluid accumulation), but because it was never filled with more than ~100 ul of water, it remained flaccid in the ventricle with negligible error due to the intrinsic stress strain characteristics of the latex. Developed pressure (peak systolic pressure minus end diastolic pressure), heart rate and coronary flow were continuously recorded over the course of each experiment and the rate pressure product (heart rate x developed pressure) was calculated as an index of myocardial work. Coronary flow was monitored by collecting the effluent from the waste line from the NMR tube containing the heart and bath and correcting for the bath flow rate of 35 ml/min. In some

experiments coronary flow was monitored by a flow meter positioned immediately prior to the point of inflow of perfusion buffer to the heart.

2.2 Shift Reagents

A stock solution of the shift reagent anion, DyTTHA^{3-} was prepared from H_6TTHA (Sigma) and $\text{DyCl}_3 \cdot 6\text{H}_2\text{O}$ (Alpha), as the Na^+ salt ($\text{Na}_3\text{DyTTHA} \cdot 3\text{NaCl}$) for addition to the Krebs-Henseleit buffer, or as the HTris salt ($(\text{HTris})_3\text{DyTTHA}$) for addition to the mannitol bathing solution. The methods for shift reagent preparation were as described by Chu *et al.* (1984).

2.3 Perfusion Buffers

Four different Krebs-Henseleit buffers were used to perfuse the hearts in the various protocols (Table 2.1). The total free sodium in a 10 mM solution of the DyTTHA^{3-} sodium salt was not 60 mM as predicted from the formula above, when measured using the Nova 6 ion analyser, but was approximately 40 mM at pH 7.40. Consequently the NaCl concentration added to the KHS buffer was 78 mM and the LKHS buffer contained 78 mM LiCl. In buffers containing the shift reagent DyTTHA^{3-} , the CaCl_2 concentration was increased to 3 mM to compensate for the binding of Ca^{2+} to DyTTHA^{3-} giving a free Ca^{2+} concentration of 1.25 mM. The presence of DyTTHA^{3-} did not affect the free concentrations of other cations in the buffer. All ion concentrations were verified using a Nova 6 ion-sensitive electrode analyser. Buffer osmolalities were between 279 and 309 mOsm.

Table 2.1: Composition of Perfusion Buffers (mM)

	KH	LKH	LKHS	KHS	Choline KH	KCl KH
NaCl	118	40	-	78	52	118
KCl	4.7	4.7	4.7	4.7	4.7	20
LiCl	-	78	78	-	-	-
MgSO ₄	1.2	1.2	1.2	1.2	1.2	1.2
CaCl ₂	1.75	1.75	3.0	3.0	1.75	1.75
Na ₂ EDTA	0.5	0.5	0.5	0.5	0.5	0.5
NaHCO ₃	25	25	25	25	25	25
Glucose	11	11	11	11	11	11
DyTTHA ³⁻	-	-	10	10	-	-

2.4 Bathing Solutions

In order to reduce any lithium signal arising from the 8.3 ml bath surrounding the heart, hearts were bathed with the fourth Krebs Henseleit buffer which contained shift reagent, but no lithium (KHS). This shifted or removed lithium signal arising from the perfusate flowing from the heart to the bath. For ²³Na NMR experiments in which the sodium signal from the bath had to be minimized, the hearts were bathed with a sodium-free, shifted mannitol solution. This solution contained 230 mM mannitol, 10 mM (HTris)₃DyTTHA and 4 mM Tris and had a pH of 7.3. It contained no cations. All bathing solutions were maintained at 37°C and flowed

around the heart at 35 ml/min, using a separate pumping system, giving a bath turnover rate of 4.2 times/min.

2.5 Washout Solutions

For the experiments in which the hearts were freeze-clamped and the intracellular cations analyzed by atomic emission spectroscopy (see below), it was necessary to flush out the extracellular space to remove any perfusion buffer that remained at the end of the experiments. In the initial experiments, the KH buffer was used to flush the extracellular space, but this necessitated correcting for the extracellular sodium and potassium concentrations. In later experiments, a 0.35 M sucrose and 5 mM histidine solution at pH 7.4 and 5°C was used to remove the perfusion buffer from the extracellular spaces (Tani and Neely, 1989). The sucrose and histidine solution was delivered by a separate perfusion line to the heart and the extracellular space was flushed for 1 min with 15 ml of solution.

2.6 External Standards

Two external standards were used to quantify the myocardial lithium and sodium concentrations and one standard was used to quantify phosphorus metabolite concentrations. The first reference solution was a concentrated dysprosium tripolyphosphate ($\text{Dy}(\text{PPP})_2^{7-}$) solution containing 12.5 μmoles of lithium and 11.3 μmoles of sodium in polyethylene tubing in a 50 μl volume. The second external standard was a thullium tetraazacyclododecane-tetramethylenephosphonate ($\text{Tm}(\text{DOTP})^{5-}$) solution containing 7.0 μmoles of lithium and 8.2 μmoles of sodium, in a 41 μl volume. The standards were attached to the bath line in the same NMR sensitive volume as the heart. The phosphorus external standard was 30 μl of a 500 mM

solution of methylphosphonic acid (15 μ moles of MPA) in a glass ball that was placed in the right atrium of the heart.

2.7 NMR Spectroscopy

Spectra were obtained using a Bruker AM 360 wide-bore NMR spectrometer (8.34T) and a 20 mm Bruker broadband probe, operating at 139.96 MHz for ^7Li , 95.25 MHz for ^{23}Na and 145.75 MHz for ^{31}P . The B₀ inhomogeneity was reduced by shimming the proton signal to 27 ± 5 Hz.

Fully relaxed lithium spectra were obtained using a pulse angle of 90° , a pulse width (PW) of 30 μs , a receiver delay (RD) of 45 s, number of scans (NS) set to 4 and 4K data points. This gave a time resolution of 3 min. Prior to Fourier transformation, the data were broadened with an LB of 10 Hz for resolution enhancement. Sodium spectra were acquired using a 90° pulse with PW = 32 μs , RD = 0.09 s, NS = 480 and 2K data points, which gave a time resolution of 2 min. Phosphorus spectra were acquired with a 60° pulse, with a PW = 24 μs , RD = 2.13 s, NS = 104 and 4K data points, providing a time resolution of 4 min.

2.8 Inductively Coupled Plasma Atomic Emission Spectroscopy (ICP-AES)

Langendorff perfused hearts were clamped between ripple-faced Wallenberger clamps previously cooled in liquid nitrogen and rapidly submerged in a small dewar of liquid nitrogen. The samples were transferred under liquid nitrogen to a -70°C freezer until they could be prepared for atomic emission spectroscopy. Heart tissue samples were freeze-dried and weighed. The samples were digested in sub-boiling, distilled, concentrated HNO_3 and then dried overnight in Teflon reaction vessels. The samples were then further solubilised in concentrated HNO_3 and HClO_3 , cooled and evaporated. Matrix matched standards were run at

the same time as the duplicated sample solutions resulting from the digestion procedure and were quantitatively analyzed by ICP-AES. The values from replicate samples were averaged and these averaged values were used to calculate mean values between hearts.

2.9 Statistical Analysis

All data presented here represent the means and standard deviations. Statistical analyses were performed using a standard one-way ANOVA and if significant, further differences were tested using a modified t-test. A two-way ANOVA with repeated measures or a split plot analysis of variance and covariance with repeated measures was used for time course experiments. Significance was set to the 95 confidence interval ($p < 0.05$) unless otherwise stated.

CHAPTER THREE
LITHIUM RELAXATION PARAMETERS

3.1 Introduction

3.2 Methods

3.3 Results

3.4 Discussion

3.1 Introduction

NMR spectroscopy makes use of the fact that certain nuclei with a quantum spin number of $1/2$ or $3/2$ lose a detectable amount of energy when placed in a magnetic field because the magnetic moments of the nuclei align with the field and the nuclei transfer energy to other nuclei, to motion, to their surroundings or to paramagnetic molecules. The simplest NMR experiment uses a single radio-frequency pulse of energy to cause the net magnetisation of the nuclei to rotate 90° into the x-axis of the magnetic field. The nuclei relax back to their starting position along the z-axis by dispersing energy into their surroundings and to other nearby molecules. The rate at which the nuclei disperse their energy to their surroundings and return to a z-axis orientation is the longitudinal or spin-lattice relaxation (T_1) time. The rate at which the NMR signal diminishes in the xy-plane is the spin-spin or transverse relaxation time (T_2). In all biological systems, the $T_2 < T_1$. In aqueous solutions, T_1 can equal T_2 if all the nuclei relax purely by dipole-dipole interaction mechanisms.

The T_1 values are usually determined by a technique called inversion recovery. A 180° pulse is applied, a variable delay (VD) time is used, a 90° pulse is applied and the signal is acquired. After a delay of ~ 5 times the expected T_1 , the sequence is repeated using several different delay times. The decay of the magnetization usually fits the following equation where M is the magnetization, M_0 is the starting magnetization, t is the time the magnetization is allowed to decay following the radio-frequency pulse and T is the time constant of the decay:

$$M = M_0(1 - e^{-t/T}) \quad (1)$$

The T_2 values can be determined using either the Carl-Purcell-Meiboom-Gill or the Hahn Spin Echo pulse sequences. Both of these techniques follow the magnetization decay in the xy plane and can be used to construct a decay curve using equation 1.

The mechanism of relaxation for a spin $1/2$ nucleus is mainly through dipole-dipole interactions, whereas for a spin $3/2$ nucleus there is an additional quadrupolar relaxation

mechanism (Woessner 1989). In the perfused heart, the nuclei also interact with charged membranes and proteins in and around the myocytes, with the consequence that T_1 and T_2 relaxation times may be important in understanding the heart at the molecular level.

3.2 Methods

3.2.1 Determination of Lithium Relaxation Parameters

The relaxation times for lithium in buffer with and without shift reagent, were estimated on LKHS buffer in a 10 mm o.d. NMR tube, inside a 20 mm o.d. NMR tube containing LKH buffer. These estimations were repeated 7 times.

In the perfused heart preparation, the heart and cannula were placed inside a 20 mm NMR tube and the cardiac effluent was suctioned from above the heart. The heart was submerged in KH buffer flowing at 35 ml/min to reduce the lithium signal arising from the bath. T_1 , T_2 and NOE measurements were made on the combined unshifted intra- and extracellular lithium, on the shifted extracellular lithium and on the intracellular lithium. T_1 measurements were estimated from inversion recovery and saturation recovery techniques (180° -VD- 90° -acquire-RD) and T_2 measurements were made using both the Carr-Purcell-Meiboom-Gill (CPMG) pulse sequence (RD- 90° -(VD- 180° -VD)*C-acquire) and the Hahn Spin-Echo sequence (RD- 90° -VD- 180° -VD-acquire). VD is a variable delay time and RD is the recycle delay (which is ~ 5 times the estimated T_1) and C is the number of times that part of the pulse sequence is repeated. An RD of 45 s was used for the perfused heart and 150 s for the buffers alone, to allow for full relaxation. The Hahn Spin Echo pulse sequence used variable delay times ranging from 1 ms to 2 s for the hearts and 1 ms to 40 s for the buffers. The CPMG had variable delays ranging from 10 ms to 2 s and 10 ms and 40 s for the hearts and buffers, respectively. An average of 18 points were collected in the construction of each

relaxation curve. Each point was a Fourier transformed lithium FID acquired with $NS = 4$, $SW = 7000$ and $TD = 4K$. The Nuclear Overhauser Enhancement (NOE) constant was determined by continuously irradiating (CW mode) the proton signal at 1.5 watts. The resultant signal was then compared to the uncoupled signal.

3.2.2 Experimental Protocol

Rat hearts were perfused at a constant pressure of 100 mmHg and maintained at a constant temperature of 37°C. Initially, the hearts were perfused with the standard phosphate-free Krebs for 10 min to ensure that the cardiac function and coronary flow were normal. They had an end diastolic pressure of 5-10 mmHg, a peak systolic pressure of 60 ± 12 mmHg, a developed pressure of 53 ± 11 mmHg, a heart rate of 311 ± 53 bpm, giving a rate pressure product of $16,054 \pm 2,182$ and a coronary flow of 17 ± 3 ml/min.

To determine the combined intra- and extracellular lithium relaxation values, the perfusion buffer was then changed to LKH for 10 min while the heart was submerged in KH buffer. During perfusion with LKH buffer, myocardial contractile function increased by 114%, described more fully in Chapter 5, and then remained stable throughout the experimental protocol. After the initial 10 min perfusion, the lithium peak area remained relatively constant and NOE ($n = 3$) or T_1 ($n = 3$) or T_2 ($n = 3$) measurements were made (Table 3.1). Upon completion of these combined intra- and extracellular lithium relaxation measurements, the heart was arrested in diastole by perfusion with the LKH buffer containing 20 mM KCl in order to close the fast sodium channels and prevent lithium movement from the intracellular to the extracellular spaces. Once the heart was fully arrested, the extracellular space was washed out with KH buffer for 1 minute and flows to both the heart and the bath were stopped. In this static, no-flow state, the intracellular T_1 ($n = 6$), T_2 ($n = 4$) and NOE ($n = 3$) measurements were performed. T_1 and T_2 measurements could not be made on the same

heart because of the length of time required to perform the pulse sequences with an adequate number of variable delay times.

A similar protocol was used to determine the lithium relaxation times in the heart in the presence of the shift reagent DyTTHA^{3-} . Following the initial perfusion with the KH solution, hearts were perfused with LKHS buffer for 10 min while submerged in the KHS bath, flowing at 35 ml/min. The hearts were then arrested by perfusion with the shifted lithium Krebs buffer containing 20 mM KCl. Once the hearts were fully arrested, all flow to both the heart and bath was stopped. T_1 or T_2 measurements were made on the unshifted intracellular peak ($n = 4$, $n = 3$) and on the shifted extracellular peak ($n = 5$ for both). NOE measurements were not made in this case because the presence of shift reagent minimized the effect of dipole-dipole coupling between the lithium and protons.

Table 3.1: Perfusion conditions used for the measurement of lithium relaxation times in heart

	-SR	+SR
Intracellular	LKH perfused/ KCl arrested heart (ischemic)	LKHS perfused/ KCl arrested heart (ischemic)
Intra & Extracellular	Normal perfusion with LKH	
Extracellular		Normal perfusion with LKHS

SR: Shift reagent $\text{Dy}(\text{TTHA})^{3-}$ LKH: Krebs Henseleit buffer (containing 78 mM Li and 78 mM Na)

LKHS: LKH with 10 mM $\text{Dy}(\text{TTHA})^{3-}$

3.2.3 Data Analysis

Each spectrum was exponentially multiplied by 5 Hz, Fourier transformed and normalized on a fully relaxed spectrum before the peak intensities were recorded using the Bruker routine. Lithium has a relatively long relaxation time so the effects of the small instrumental delays were negligible. The T_1 data were fitted to a single exponential using the standard Bruker software. In the cases where the data fitted a mono-exponential equation, the T_2 values were determined using the standard Bruker software. If the T_2 data did not fit a single exponential, they were fitted to a double exponential using the equation

$$M = M_0(Ae^{-t/a} + Be^{-t/b}) \quad (2)$$

where $A + B = 1$, and A represents the fraction of total signal decaying with the fast time constant a and B represents the fraction of total signal decaying with the slow time constant b. The NOE values (η) were determined using the formula

$$\eta + 1 = \frac{\text{SATURATED}}{\text{UNSATURATED}} \quad (3)$$

Data are presented as the means \pm SD.

3.3 Results

3.3.1 Lithium in Buffer

The T_1 and T_2 relaxation times for lithium in Krebs-Henseleit buffer were 25 s and 19 s respectively (Tables 3.2 and 3.3). Both were calculated from data that fitted mono-

exponential equations. In the presence of the shift reagent DyTTTHA^{-3} , the T_1 and T_2 relaxation times for lithium were shortened ~ 38 -fold to 0.65 s and 0.49 s (Table 3.3). Again, both were calculated from data that fitted mono-exponential equations.

3.3.2 Lithium in Perfused Heart

In the hearts perfused with LKH buffer, the lithium spectrum consisted of a single, narrow peak with a line width at half height of ~ 16 Hz representing both the intra- and extracellular pools of lithium (Fig. 3.1a). Use of shift reagent in the perfusion buffer caused the lithium peaks to broaden to a line width of ~ 30 Hz, but allowed the discrimination of intra- and extracellular lithium. The lithium spectrum, obtained after 20 min perfusion

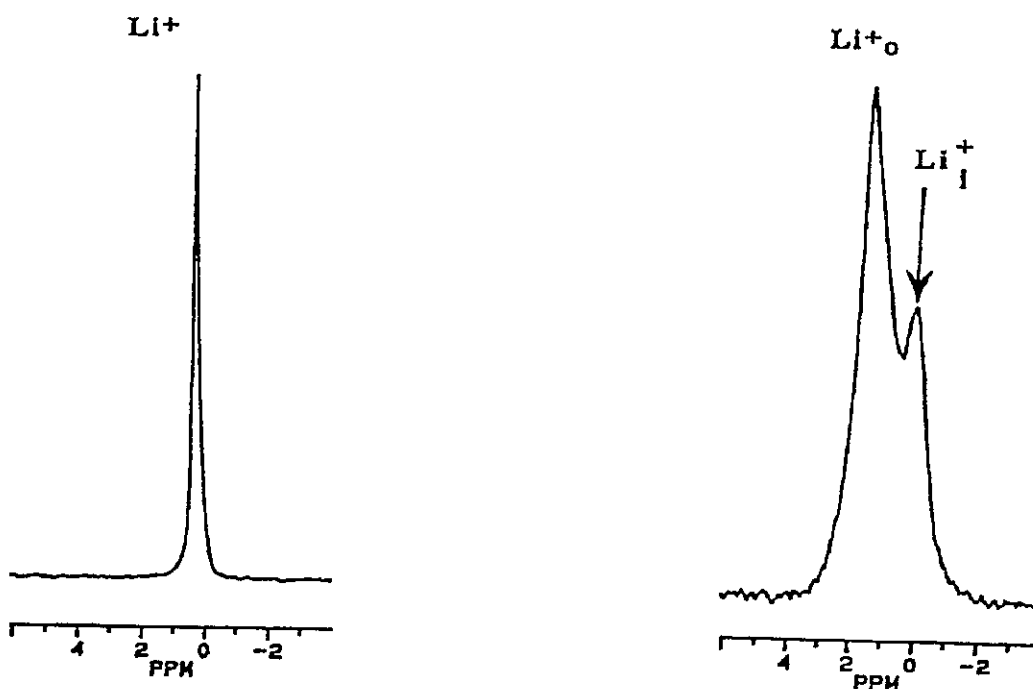


Figure 3.1: a) A lithium spectrum from an isolated, rat heart perfused with LKH buffer
b) The same heart perfused with LKHS buffer.

with the LKHS buffer, consisted of a large shifted peak on the left, representing the extracellular lithium and a smaller unshifted peak representing the intracellular lithium (Fig. 3.1b).

The T_1 of the unshifted lithium resonance was a combination of both the intra- and extracellular resonances with the extracellular contribution being dominant because of the larger extracellular volume. The T_1 was found to be 6.8 s and was calculated from data that fitted a mono-exponential equation. The T_2 data was best fitted by a bi-exponential

Table 3.2: Lithium T_1 values in perfusion buffer and the perfused rat heart (s)

	-SR	+SR
Perfusion Buffer	25 ± 0.5	0.65 ± 0.05
Perfused Heart		
Intracellular	9 ± 2	7.5 ± 0.4
	(n = 6)	(n = 4)
Intra & Extracellular	6.8 ± 0.2	
	(n = 3)	
Extracellular		0.6 ± 0.1
		(n = 5)

SR: Shift reagent $\text{Dy}(\text{TTHA})^{3-}$ Data are presented as means \pm SD

equation having a fast component of 0.17 s and a slow component of 0.85 s. The ratio of the fast to slow components was 0.65:0.35. In the presence of shift reagent, the T_1 of extracellular lithium was considerably shortened to 0.6 s and the T_2 was 0.41 s (Tables 3.2 and 3.3). Both were calculated from data that fitted mono-exponential equations.

Table 3.3: Lithium T_2 values in perfusion buffer and in the perfused rat heart (s)

		-SR	+SR
Buffer		19 ± 1	0.49 ± 0.04
Perfused Heart			
Intracellular	fast	0.04 ± 0.02	0.029 ± 0.001
	slow	1.12 ± 0.04	1.2 ± 0.3
	<i>fast:slow</i>	<i>45:55</i>	<i>89:11</i>
		(n = 4)	(n = 3)
Intra &			
Extracellular	fast	0.17 ± 0.02	
	slow	0.85 ± 0.52	
	<i>fast:slow</i>	<i>65:35</i>	
		(n = 3)	
Extracellular			0.41 ± 0.13
			(n = 5)

SR: Shift reagent Dy(TTHA)³⁻ Data are presented as means \pm SD

Intracellular lithium demonstrated mono-exponential relaxation, giving a T_1 of 9 s and a bi-exponential T_2 having a fast component of 0.04 s and a slow component of 1.12 s in the ratio 0.45:0.55. With shift reagent in the extracellular buffer (but not in the intracellular space) the intracellular T_1 was 7.5 s and the T_2 was again biexponential, having a fast component of 0.029 s and a slow component of 1.2 s. In this case though, the ratio of the fast to slow components was 0.89:0.11 (Tables 3.2 and 3.3).

NOE values were calculated for the lithium peak in hearts perfused with LKH and for the intracellular peak alone in KCl arrested ischemic hearts. The ratio of the saturated to unsaturated peak areas gave an η of 0.50 ± 0.17 for both unshifted peaks.

3.4 Discussion

Lithium is a spin 3/2 nucleus with a relatively weak nuclear electric quadrupole moment compared to sodium and potassium. The interaction between the quadrupole moment and the local electrostatic field gradients constitute the primary relaxation mechanism for lithium. Dipole interactions between lithium ions and protons also provide an alternate relaxation mechanism. We found unshifted lithium in heart has a 50 % increase in signal intensity upon saturating, indicating a substantial contribution of dipole-dipole coupling to lithium relaxation.

Lithium is able to enter heart cells by moving down its electrochemical gradient until it equilibrates with the lithium concentration in the extracellular perfusion buffer. The intra- and extracellular pools of lithium ions combine to give a single peak which is 75% extracellular, due to the larger extracellular volume in the perfused heart (Clarke *et al*, 1988). Any contributions to the signal from lithium passing into the bath from the heart were minimized by continuously washing around the heart with lithium-free Krebs buffer.

The T_1 for lithium in aqueous Krebs Henseleit solution at 37°C was approximately 25 s while the T_2 was 19 s giving a T_1/T_2 of ~ 1.3 (Table 3.4). In the presence of shift reagent, the

T_1 and T_2 values decreased to less than 1 s but the T_1/T_2 ratio remained at ~ 1.5 (Table 3.4). This is consistent with the extreme narrowing condition in which $T_1 \cong T_2$ and is in keeping with previously reported values for lithium in solution (Burstein and Fossel, 1987; Woessner, 1989; Gullapalli, 1990).

In the absence of shift reagent, the lithium perfused heart has a single combined intra- and extracellular peak. The T_1 of this peak has a value of 6.8 s, which is not significantly different from the intracellular lithium T_1 of 9 s ($p > 0.05$). To measure the intracellular T_1 's, the hearts were in an arrested, ischemic state with minimal lithium efflux across the sarcolemmal membrane. Dissolved O_2 acts as a paramagnetic relaxing agent and thus shortens relaxation times (Woessner, 1989). The decrease in the total amount of oxygen present during ischemia increased the relaxation time of the intracellular lithium and resulted in their higher mean T_1 of 9 s and greater range of measurements (7.1 - 11.9 s). The presence of shift reagent in the extracellular space had no effect on the intracellular T_1 values. The shifted extracellular lithium ions exhibited a T_1 that was the same as the shifted buffer alone, indicating that lithium binding in the extracellular space was minimal and exchange of lithium across the sarcolemma was slow on the NMR time scale.

The T_1/T_2 ratios increased 100-fold, from 1.3 for lithium in the buffer alone, to approximately 130 for intracellular lithium (Table 3.4). This indicates that the correlation time for intracellular lithium is much longer than for free lithium in buffer.

In all cases, the T_2 values were significantly shorter than the T_1 values. In the buffers and in the shifted extracellular buffer, the T_2 decay curves were all mono-exponential. The intracellular T_2 's data were best fit by bi-exponential equations. The fast and slow components differed by two orders of magnitude and had relative amplitudes of 0.45 and 0.55 respectively. This is close to the theoretical values of 0.4 and 0.6 predicted from an homogeneous pool of nuclei undergoing quadrupolar interactions. The presence of shift reagent in the extracellular space did not alter the fast and slow time constants for intracellular lithium, but it did affect

their relative amplitudes, increasing that of the fast component and decreasing that of the slow component. The effect on the amplitudes may have been due to the close proximity of the large, paramagnetic shift reagent molecules on the other side of the cell membrane that were able to exert bulk magnetic susceptibility effects (Chu, 1990) on the lithium ions close to the membrane without affecting the centrally located ions.

Table 3.4: Lithium T_1/T_2 values in perfusion buffer and the perfused rat heart

	-SR	+SR
Perfusion Buffer	1.3	1.5
Perfused Heart		
Intracellular	113	298
Intra & Extracellular	28	
Extracellular		1.3 (n = 5)

SR: Shift reagent Dy(TTHA)³⁻

Bi-exponential T_2 values have been reported for intracellular sodium ions in heart (Burstein and Fossel, 1987) and red blood cells (Shinar and Navon, 1984) and a lengthening of correlation times has been reported for both sodium and lithium (Pettegrew *et al.*, 1987; Gullapalli *et al.*, 1990; Burstein and Fossel, 1987). Several hypotheses have been put forward to explain this phenomenon, including:

1. the relative immobilization of cations by the transient binding to negatively charged intracellular macromolecules,
2. a fast exchange between two pools of nuclei with different relaxation times and
3. the diffusion of the cation through fluctuating local electrostatic field gradients.

Due to the inhomogeneous nature of the intracellular compartment, it is unlikely that a single cause for the alteration in lithium relaxation behavior could be determined and theoretical predictions of these relaxation parameters are unable to account for all the above factors.

In summary, we have found the relaxation times for lithium to be long, both in buffer and in the intra- and extracellular spaces of the heart and that dipole interactions account for a significant amount of lithium relaxation. The longitudinal relaxation time curves (T_1) were mono-exponential and the intracellular transverse (T_2) relaxation times were bi-exponential. There was a large increase in the correlation time in the perfused heart compared to the perfusion buffer, probably due to the interaction of lithium with anionic, intracellular macromolecules.

CHAPTER FOUR
LITHIUM WASH-IN AND WASHOUT KINETICS
AND
LITHIUM UPTAKE DURING ISCHEMIA

4.1 Introduction

4.2 Methods

4.3 Results

4.4 Discussion

4.1 Introduction

Lithium movements across cell membranes have been characterized in red blood cell suspensions, in superfused atrial and ventricular tissue samples and on frog sartorius muscle, but they have not been studied in the intact, beating, mammalian heart under physiological conditions. Differences in temperature, perfusion techniques and tissue viability have led to a wide range of values for the influx and efflux rates of lithium movement across a cell membrane. In red blood cell preparations (Pettegrew *et al.*, 1987 and Gullapalli *et al.*, 1990), in frog sartorius muscle (Keynes and Swan, 1959, Yonemura and Sato, 1967) and in superfused heart tissue (Lullman *et al.*, 1990), the rates of lithium movements across the membrane are of the order of mM/hour. The different rates in these studies, reflect differences of tissue preparations, channel and exchanger activities, temperature and cell type, therefore it was important for us to investigate the kinetics of lithium movements in our experimental model; the functioning, perfused rat heart. The kinetics of lithium movements across the sarcolemma in the normal and ischemic rat heart were followed using ^7Li NMR spectroscopy before specific channel and exchange inhibitors were used to further characterize the mechanisms of sodium and lithium transsarcolemmal movements during ischemia.

4.2 Methods

4.2.1a Wash-in and Ischemia Protocols

Isolated rat hearts ($n = 3$) were perfused with Krebs Henseleit (KH) buffer at 37°C for 20 min to ensure that myocardial function and flow were normal. To determine the kinetics of the movement of lithium into the intracellular space during perfusion and ischemia, the following protocol was followed: The perfusion buffer to the heart was switched to a modified

Krebs Henseleit buffer containing 78 mM lithium, 78 mM sodium and 10 mM DyTTTHA³⁻ (LKHL). At the same time, the heart was surrounded by KH bath containing 10 mM DyTTTHA³⁻ (KHS), flowing at 35 ml/min. The bath was used to minimize the lithium signal arising from the perfusate leaving the heart, with the result that > 90% of the lithium signal was from the heart itself (Anderson *et al.*, 1991). Four fully relaxed lithium spectra were acquired with NS = 8, PW = 30 ms and RD = 45 s. This gave a time resolution of 6 min and a total wash-in time of 24 min. After the 24 min LKH perfusion, the flows to the heart and the bath were turned off and the heart was subjected to 28 min global, normothermic ischemia during which four fully relaxed lithium spectra were acquired. At the end of the 28 min ischemia, the hearts were flushed with KH buffer for 30 s to remove any lithium still present in the extracellular space. A final lithium spectrum was acquired and the hearts were freeze-clamped at the temperature of liquid nitrogen. The frozen hearts were analyzed by ICP-AES to verify the final concentration of intracellular lithium at the end of ischemia.

4.2.1b Data Analysis

In the spectra from hearts perfused with LKHS, the intra- and extracellular peaks overlapped (see Figure 3b), consequently the wash-in spectra could not be fitted using the NMR1 program on the Sun computer. Therefore spectra were quantified by measuring the height and width of the intra- and extracellular lithium peaks and calculating the peak areas by triangulation. During triangulation the area of overlap between the peaks was divided in proportion to the peak areas thereby correcting for the contribution of one peak to the other. The concentrations were calculated assuming an extracellular volume of 1.42 ml/g and an intracellular volume of 0.45 ml/g (Clarke *et al.*, 1992) and assuming that the extracellular lithium concentration was the same as in the perfusion buffer. The extracellular volume in this case is the volume of the heart chambers, the interstitial space and the coronary vasculature.

The intra- and extracellular volume values of 0.45 ml/g and 1.42 ml/g were determined in ^{31}P NMR experiments using sodium phenylphosphonate as an extracellular space marker and dimethyl methylphosphonate as a total tissue space marker (Clarke *et al.*, 1992). The difference between these values yields an estimation of the intracellular volume. The intracellular lithium concentrations were determined by comparison of the intracellular peak area with that of the external reference containing 12.5 mmoles of lithium and the shift reagent $\text{Dy}(\text{PPP})_2^{7-}$. The width of the peaks at half maximum height was found to remain the same throughout the protocol, therefore peak heights were used to define the changes in lithium concentration during wash-in and ischemia.

4.2.2a Washout

To characterize the washout of intracellular lithium, hearts ($n = 3$) were first perfused with KH for 20 min to ensure that myocardial function and flow were normal. The buffer was then switched to one containing 78 mM lithium and 78 mM sodium (LKH) for 30 min to load the myocardial cells with lithium. The hearts were then perfused with lithium-free KH and submerged in a KH bath flowing at 35 ml/min. Fully relaxed lithium spectra (see acquisition parameters above) were acquired as the lithium was washed out of the myocardial intracellular spaces.

4.2.2b Data Analysis

Because the spectra consisted of single, unshifted peaks, they were fitted using the NMR1 software program on a Sun 3/160C workstation. The integral of the area under the peaks was estimated using the sum of Lorentzian and Gaussian curves to fit the peaks.

4.3 Results

4.3.1 Wash-In

The movement of lithium into the intracellular space of the heart was best described by a mono-exponential equation (Fig. 4.1) with a rate constant (k_1) of 0.068 min^{-1} , a $t_{1/2}$ of 10.3 min and an initial rate of increase of 5.27 mM/min. The intracellular lithium concentration ($[\text{Li}^+]_i$) at the end of 24 min perfusion was $57 \pm 7 \text{ mM}$, not yet having reached steady state values. Hearts subjected to the same protocol, extracted and analyzed by ICP-AES, had an intracellular lithium concentration of $50 \pm 2 \text{ mM}$ at the end of a 20 min perfusion with KHL.

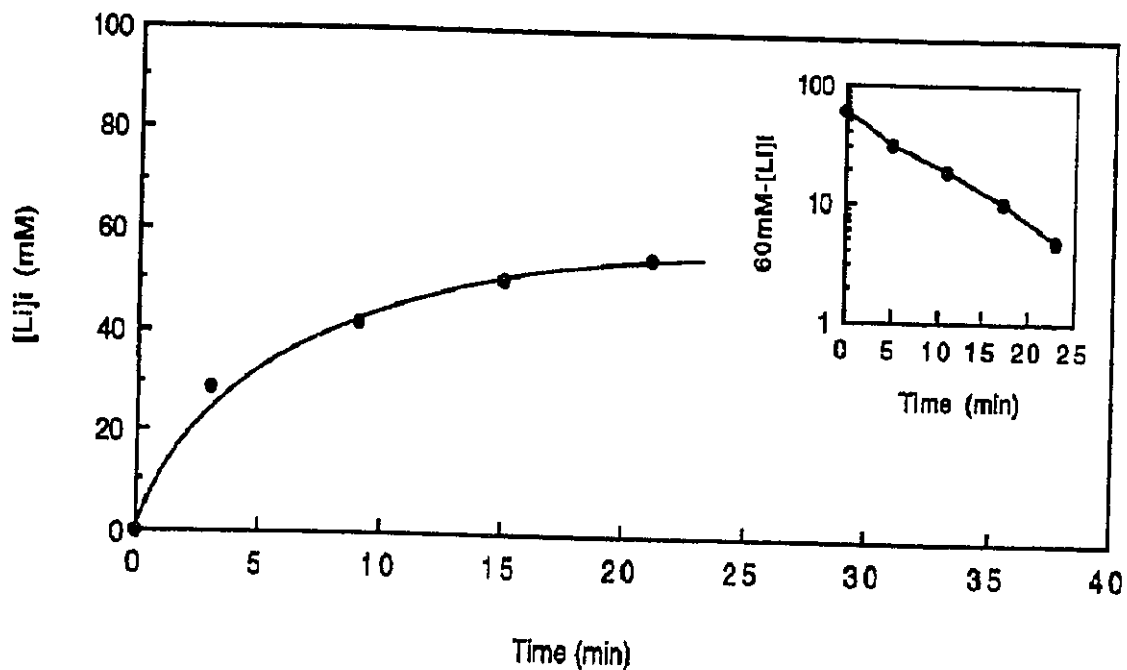


Fig. 4.1: Lithium uptake by the myocardium during perfusion with Krebs Henseleit buffer containing 78 mM lithium. Inset: semi-log plot of 60-lithium concentration versus time. The line through the points is intended to guide the eye and does not represent the equation for the line of best fit.

4.3.2 Ischemia

Lithium uptake during ischemia followed 24 min lithium wash-in and therefore started from an intracellular lithium concentration of 45-60 mM. The uptake was linear at a rate of 1.34 mM/min (Fig 4.2). At the end of the 28 min ischemia, $[\text{Li}^+]_i$ was 78 ± 10 mM. ICP-AES analysis gave a final lithium concentration of 79 ± 12 mM after 28 min ischemia.

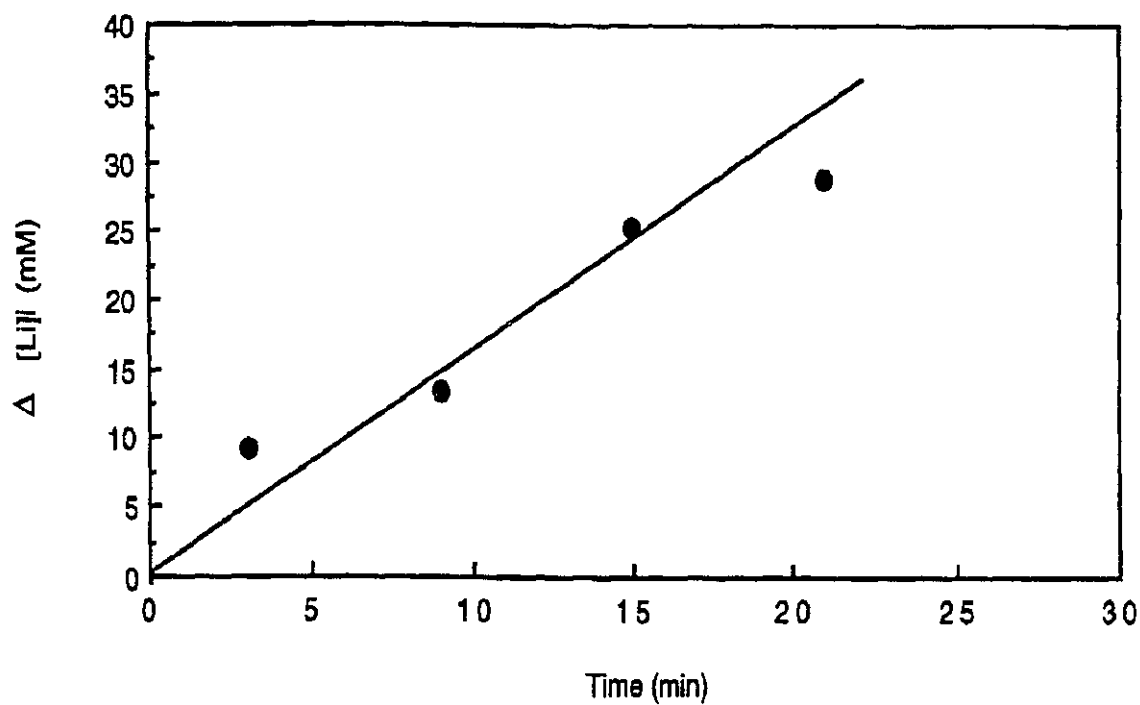


Fig. 4.2 Lithium uptake during myocardial ischemia. The line through the points is intended to guide the eye and does not represent the equation for the line of best fit.

4.3.3 Washout

The washout of lithium from the myocardium followed 30 min lithium wash-in, so it started from intracellular lithium concentrations of approximately 60 mM, determined by extrapolating the wash-in curve. The washout data were best fit by a mono-exponential equation having a k_1 of 0.062 min^{-1} , a $t_{1/2}$ of 11.2 min and an initial rate of 4.83 mM/min. The data were taken from three hearts, but the points were not averaged because slightly different time points were used (Fig. 4.3).

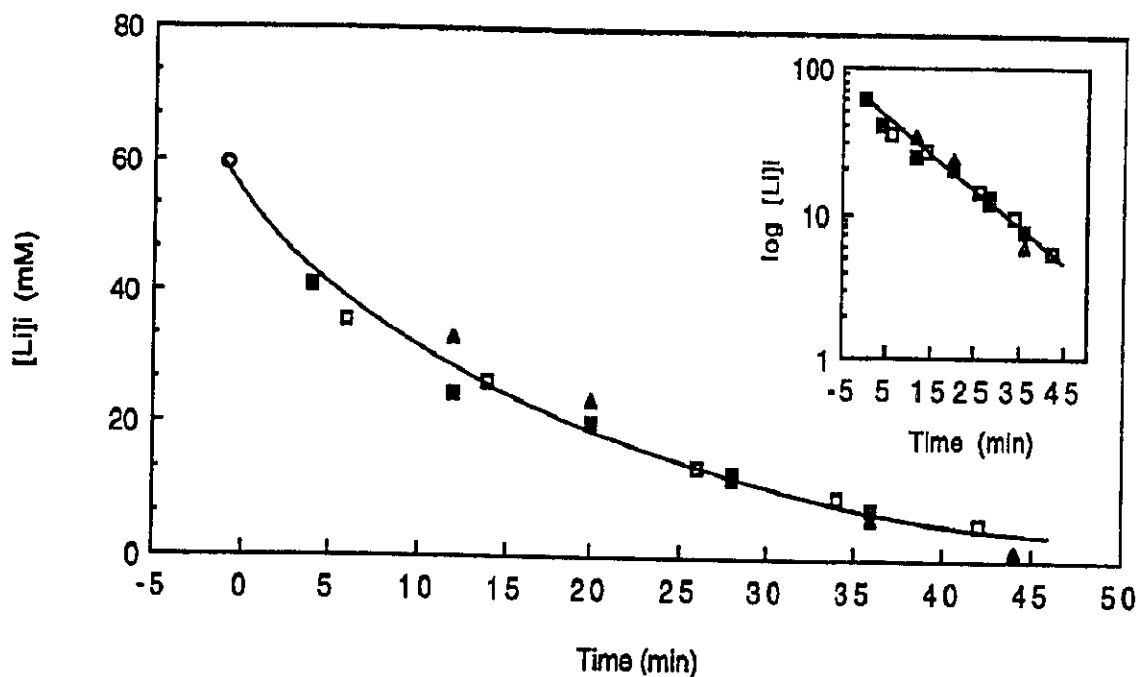


Fig. 4.3: Washout of lithium from the myocardium. The first point was determined by extrapolation of the wash-in curve (Fig. 4.1). Inset: semi-log plot of the decrease in intracellular lithium concentration versus time. The line through the points is intended to guide the eye and does not represent the equation for the line of best fit.

There was excellent agreement between the NMR and the ICP-AES analyses of the intracellular lithium concentrations in both the wash-in and ischemia protocols (Table 4.1). Lithium increased to the same extent during 48 min perfusion with LKH buffer as during ischemia. The movement of lithium into the intracellular space resulted in a 40% loss of sodium and a 34% loss of potassium from the cells in the LKH perfused hearts (Table 4.2).

Table 4.1: Intracellular Lithium Concentrations During Wash-in and Ischemia (mM)

Protocol	NMR Data	ICP-AES Data
20 min perfusion with LKH	55 ± 7	50 ± 2
28 min ischemia	78 ± 11	79 ± 12
48 min perfusion with LKH		80 ± 3

Data presented are the means \pm SD (n = 3)

Table 4.2: Intracellular Cations Concentrations in Control and Lithium Perfused Hearts
Determined by ICP-AES (mM)

Buffer	$[\text{Na}^+]_i$	$[\text{K}^+]_i$	$[\text{Li}^+]_i$
20 min perfusion with KH	23 ± 3	87 ± 5	0
20 min perfusion with LKH	14 ± 2	57 ± 5	50 ± 2

Data presented are the means \pm SD (n = 3)

4.3: Discussion

Lithium uptake into heart cells was rapid and mono-exponential with a time constant of 10.3 min (0.17 h). After twenty minutes, the intracellular lithium concentration was 55 ± 7 mM, 61 - 79 % of the equilibrium value of 78 mM. Since lithium movement across the sarcolemma is most likely an electrically neutral process, occurring via exchange of lithium with protons, sodium and potassium, its equilibrium value can be approximated by its concentration gradient. The efflux of lithium from hearts pre-loaded with LKH for 30 min was also mono-exponential and had a time constant of 11.2 min, which was almost identical to the lithium uptake time constant. The rate of lithium uptake has been studied in red blood cell suspensions by Pettegrew *et al.* (1987), who found lithium uptake was mono-exponential with a time constant of 14.7 h for red blood cells incubated in 50 mM lithium at 25°C. Gullapalli *et al.* (1990) also found the lithium uptake in red blood cells to be mono-exponential with a time constant of 16.5 h. Pettegrew and Woessner (1989) reported a lithium efflux rate of 1% per hour in red blood cells at 25°C. In 1959, Keynes and Swan examined the rate of lithium uptake in the frog sartorius muscle by soaking strips of muscle for varying periods of time, at room temperature, in a modified Ringer's solution in which all the sodium was replaced with lithium. They found a rate of lithium uptake of 0.041 - 0.079 mM/min and an efflux rate of 0.096 mM/hr, with a rate constant of 0.095 h⁻¹. In a similar series of experiments, Yonemura and Sato (1967) found a 10-fold faster rate of lithium uptake of 0.474 mM/min and an efflux rate of 0.13 mM/min with a rate constant of 0.54 h⁻¹. Our perfused hearts had a 70-130 fold faster rate of lithium influx of 5.27 mM/min, with a rate constant of 0.068 min⁻¹ (4.08 h⁻¹) and an efflux rate of 4.83 mM/min with a rate constant of 0.062 min⁻¹ (3.72 h⁻¹). Despite this range of values, all workers conclude that lithium uptake and efflux follow exponential rate equations. The differences between the results of the muscle experiments and ours can be explained by the conditions used to measure influx and efflux. The muscle strips were soaked

and not perfused, so lithium was not delivered as efficiently to the cells as in the perfused heart nor was it removed as efficiently from the extracellular spaces during efflux experiments. A study on superfused left atrial and ventricular papillary muscle, stimulated at a rate of 1 Hz at 37°C, found that the intracellular lithium equilibrated with the extracellular buffer (76 mM) after 180 min (Lullmann *et al.*, 1990). Extrapolation of our wash-in curve indicated that equilibrium would have been reached after 45 - 55 min perfusion with LKH. The increased rate of lithium influx and efflux in our experiments compared to rates found by other investigators could reflect the contributions of the fast sodium channel and of temperature to the net lithium flux across the sarcolemma. One of the main routes of lithium entry into heart cells is most likely the fast sodium channel, which opens and closes with each wave of excitation, thereby allowing a pulsed stream of lithium ions to flow across the sarcolemma. The absence of a fast sodium channel in the red blood cell membrane and the lack of stimulation in the muscle strip preparations, as well as the low stimulation rate used in the papillary muscle experiments, would decrease the contribution to lithium influx via this channel. The lower temperatures of the red blood cell and muscle strip experiments would also have decreased the rates of lithium movements across the cell membranes.

The ICP-AES data also demonstrate that as lithium is taken up by the heart cells, both sodium and potassium are lost as the cells try to maintain a normal cation concentration and osmolality. We found the cells lost ~30% of their potassium and ~40% of their sodium. This sodium and potassium loss has been observed by Keynes and Swan (1959), Yonemura and Sato (1967) and Gow and Ellis (1990). In particular, Gow and Ellis (1990), found a linear correlation between intracellular lithium gain and potassium loss. The potassium concentrations reported here were somewhat lower than expected. In a review (Polimeni, 1984), intracellular potassium values in the perfused heart ranged from 76 to 151 mM measured using radiolabel techniques; our value of 87 mM falls within this range. Using a method similar to ours Tani and Neely (1990) found intracellular potassium to be ~118 mM.

While our values are low, when used to calculate the membrane potential using the Nernst equation, they give a resting membrane potential close to the measured value. If the values are incorrect, one possible explanation is that during our flushing of the extracellular space with the cold sucrose and histidine solution, some of the intracellular potassium escaped from the cells and was washed away. The atomic emission method was accurately measured the levels of potassium in the standards run prior to the heart samples so any errors must have occurred during the flushing procedure. It should be stressed that there is a great deal of variability in the potassium concentrations estimated in the isolated perfused heart (Polimeni, 1984). The potassium concentration values reported here show qualitative changes in the intracellular potassium ion concentration. Further experiments with using ^{39}K NMR could be used to confirm the intracellular potassium concentrations.

There are a limited number of known mechanisms for lithium transport across the sarcolemma and our finding that the kinetics for lithium wash-in and washout are the same allows us to speculate as to the existence of electrically neutral Na^+/Na^+ and K^+/K^+ exchanges. If such exchange mechanisms were present and if lithium could substitute for sodium or potassium in them, it would provide one explanation for lithium equilibration across the cell membrane. The Nernst equation allows an estimation of the free energy change $\Delta G_{\text{Li/H}}$, for coupled Li^+ influx and H^+ efflux (another electrically neutral exchange that we know does take place). The equation is as follows:

$$\Delta G_{\text{Li/H}} = mF \Delta\Psi + RT \ln \left(\frac{[\text{Li}^+]_i}{[\text{Li}^+]_o} \right) - nF \Delta\Psi + RT \ln \left(\frac{[\text{H}^+]_o}{[\text{H}^+]_i} \right)$$

where m and n are the number of ions moved in each direction, F is Faraday's constant ($96.5 \times 10^3 \text{ kJ mV}^{-1} \text{ mol}^{-1}$), $\Delta\Psi$ is the resting membrane potential (-85 mV), R is the gas constant ($8.31 \times 10^{-3} \text{ kJ K}^{-1} \text{ mol}^{-1}$) and T is the absolute temperature (310 K). The membrane potential terms add to zero, because Li^+/H^+ exchange is electroneutral (i.e., $m = n$), yielding

$$\Delta G_{\text{Li/H}} = RT \left(\ln \left(\frac{[\text{Li}^+]_i}{[\text{Li}^+]_o} \right) + \ln \left(\frac{[\text{H}^+]_o}{[\text{H}^+]_i} \right) \right)$$

If one assumes the $[\text{Li}^+]_i$ is 1 mM, $[\text{Li}^+]_o$ is 78 mM, pH_i is 7.1 and pH_o is 7.4, the $\Delta G_{\text{Li/H}}$ for lithium influx via Li^+/H^+ exchange is -12.99 kJ/mol. The free energy changes for other such electrically neutral exchanges can also be calculated and are shown in Table 4.3.

Table 4.3: Free energy changes (ΔG) for electrically neutral ion exchanges during lithium wash-in

A ⁺	[A ⁺] _i (mM)	[A ⁺] _o (mM)	ΔG kJ/mol
H ⁺	7.8 x 10 ⁻⁸	4 x 10 ⁻⁸	-12.99
Na ⁺	23	78	-8.07
K ⁺	87	4.7	-18.72

If a Na^+/Li^+ or K^+/Li^+ exchanges did exist, the negative values for ΔG indicate that such changes are energetically favorable under these perfusion conditions and could have contributed to the movement of lithium into the cell. The most favorable exchange under wash-in perfusion conditions is K^+/Li^+ exchange because lithium is at a high extracellular concentration and potassium is at a high intracellular concentration. It is also possible to calculate the ΔG for reversed versions of these exchanges during washout perfusion conditions (Table 4.4). Under washout conditions the extracellular sodium concentration is 144 mM and the intracellular lithium concentration is ~60 mM so lithium efflux by Na^+/Li^+ exchange could account for a large amount of the total lithium washout especially since this mechanism is not limited by the build-up of sodium intracellularly since the sodium pump is continually extruding sodium ions from the cell.

Table 4.4: Free energy changes (ΔG) for electrically neutral ion exchanges during lithium washout

A ⁺	[A ⁺] _i (mM)	[A ⁺] _o (mM)	ΔG kJ/mol
H ⁺	7.8 x 10 ⁻⁸	4 x 10 ⁻⁸	-8.29
Na ⁺	14	144	-16.06
K ⁺	57	4.7	-3.64

The lithium uptake during ischemia was linear, at a rate of 1.34 mM/min. This is similar to the rate of 1.65 mM/min for intracellular sodium increase during ischemia reported by Anderson *et al.* (1990). The large changes in intracellular ions during ischemia may result in changes in volume, but it is not possible to measure such volume changes in the ischemic heart. Consequently, the concentration changes during ischemia reported here were calculated assuming a constant intracellular volume. The fast sodium channels are closed during ischemia (Poole-Wilson *et al.*, 1984) consequently the lithium uptake probably occurred predominantly via Li⁺/H⁺ exchange, which would have been stimulated by the increase in intracellular proton concentration produced during anaerobic glycolysis. It is possible to show that sufficient protons are generated from anaerobic glycolysis during ischemia. The glycogen content of the rat heart is ~20 μ moles of glucose equivalents/g wet weight so, with an intracellular volume of 0.45 ml/g wet weight the intracellular concentration is 45 mM. It has been shown that ~90-100% of the total glycogen is converted to glucose-6-phosphate during 28 min global ischemia (Nedelec, 1992). For every glucose-6-phosphate used in anaerobic energy production, two lactates and three protons are produced: so for 45 mM glucose-6-phosphate (from glycogen), 90 mM lactate and 135 mM protons would be generated (Opie, 1991). Even if all the lactate produced moves out of the cells via a H⁺/lactate⁻ cotransport mechanism and one allows for a 36 mM/pH unit buffer capacity of the cells (Nedelec *et al.*, 1992), there would still be a 45 mM

increase in proton concentration able to drive Li^+/H^+ exchange and thereby account for the uptake of lithium during ischemia.

It was surprising that intracellular lithium increased to the same extent during a 48 min perfusion with LKH buffer as during 28 min ischemia. During a 48 min perfusion with LKH buffer, the large proton pool from anaerobic glycolysis would not have been available for exchange with lithium so the intracellular lithium increase must have occurred predominantly via lithium movement through the fast sodium channels. Again, Na^+/Li^+ or K^+/Li^+ exchanges could have operated both during the 48 min perfusion with LKH and during ischemia but later experiments with the Na^+/H^+ exchange inhibitor, amiloride (see Chapter 6), indicate that the existence of these exchangers is unlikely or if they do exist, they must also be inhibited by amiloride. In each case, lithium equilibrated according to its electrochemical gradient across the sarcolemma. In further experiments, it would be of interest to enter ischemia from a lower intracellular lithium concentration to observe the lithium uptake from a point further away from its equilibrium value.

The close agreement between the NMR and ICP-AES results indicate that lithium in the heart is 100% NMR visible. Visibility of the sodium cation in the intracellular environment has been a subject of much controversy (Springer *et al.*, 1987., Malloy *et al.*, 1990., Pike *et al.*, 1985). In most studies, the intracellular sodium concentrations determined by NMR spectroscopy were much less than those determined by atomic emission spectroscopy but this could be due to the short relaxation times for sodium with the result that the spectrometer is unable to acquire the signal fast enough, resulting in an apparent NMR "invisible" pool of sodium ions. In our studies ^7Li NMR visibility would not be a problem since lithium relaxation times are so long. It is unlikely that the visibility differences reflect a difference in the cellular binding characteristics of sodium and lithium. Intracellular lithium appears to be present as a free cation in the intracellular matrix, binding transiently, if at all, to negatively charged macromolecules, being neither bound nor sequestered in intracellular organelles.

In summary, lithium equilibrates across the sarcolemma according to its electrochemical gradient, as evidenced by the fact that the intra and extracellular lithium concentrations approach the same value during wash-in and washout studies. In the process, lithium displaces 30% of the intracellular potassium and 40% of the sodium. Once inside the cell, the lithium cation remains free and NMR visible. Lithium has a rate of uptake during ischemia that is similar to the rate of sodium uptake, therefore it can serve as a useful probe to characterize the mechanisms by which sodium increases during ischemia.

CHAPTER FIVE
CARDIAC FUNCTION AND ENERGETICS DURING LITHIUM PERFUSION

5.1. Introduction

5.2 ³¹P NMR Spectroscopy

5.3 Bench Experiments

5.4 Results

5.5 Discussion

5.1. Introduction

The transmembrane sodium gradient is of key importance to the function and viability of excitable cells, such as heart cells. The consequences of lowering this gradient by decreasing the extracellular sodium concentration include, alterations in the shape and duration of the action potential (Niedergerke and Orkands, 1966), a small decrease in the heart rate and a large increase in contractile function due to an increase in intracellular calcium levels (Kolar *et al.*, 1990).

In the experiments described in Chapter 3, a sustained increase in contractile function was observed on perfusion with LKH buffer (78 mM sodium and 78 mM lithium). Such a large increase in workload would be expected to increase the ATP and PCr demand of the heart and could possibly result in a decrease in the steady state levels of these phosphorus compounds. Consequently, we investigated the metabolic effects of these functional changes using ^{31}P NMR spectroscopy.

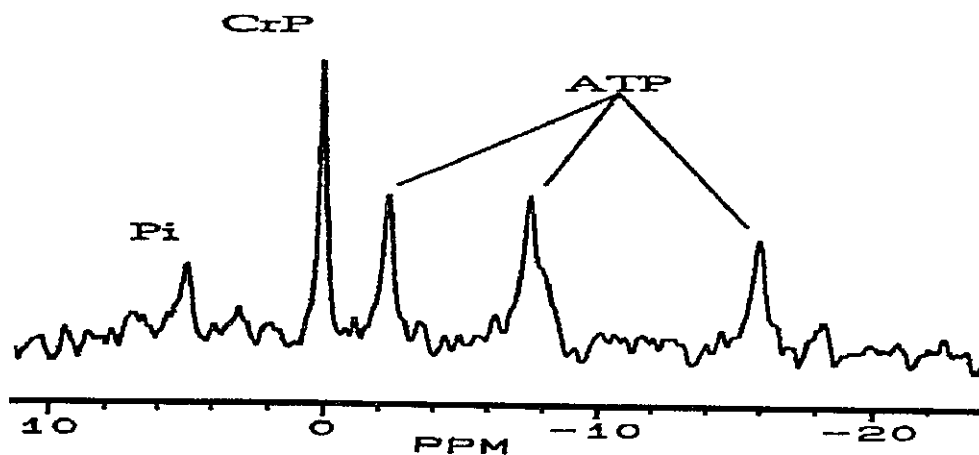


Fig. 5.1: ^{31}P NMR spectrum of an isolated, perfused rat heart.

Using ^{31}P NMR spectroscopy, changes in the levels of the high energy phosphate metabolites, phosphocreatine (PCr), adenosine triphosphate (ATP) and inorganic phosphate (Pi) (Fig. 5.1), as well as intracellular pH, were observed and correlated with alterations in the intracellular ionic content, determined by atomic absorption (ICP-AES).

5.2 ^{31}P NMR Spectroscopy

5.2.1 Lithium Perfusion for 48 minutes

In order to establish the metabolic and functional stability of the rat heart perfused with LKH, hearts ($n = 4$) were perfused for times equivalent to the ischemia/reperfusion protocol. Hearts were perfused with KH buffer for 20 min. Heart rate, end diastolic pressure and peak systolic pressure were monitored by placing a water-filled latex balloon into the left ventricle via a small opening in the left atrial appendage. The balloon was connected to a Gould pressure transducer and recorder and filled to a with ~ 100 ul of water to achieve an end diastolic pressure of 5-10 mmHg. The changes in pressure and heart rate allowed the rate pressure product to be calculated. Myocardial flow was measured at the same time as the function trace was examined, by either collecting the effluent from the heart in a graduated cylinder for 1 min intervals or by taking the measurement from a flow meter positioned just above the point of entry of the perfusion line in the cannula apparatus. Two 4 min phosphorus spectra were acquired with an NS = 104, PW = 32 ms and RD = 2.15 s. The perfusion buffer was then switched to LKH for 48 minutes and twelve more ^{31}P spectra were acquired and function and flow measured.

5.2.2 Ischemia and Reperfusion

Hearts ($n = 4$) were perfused with KH buffer for 20 min. Heart rate, end diastolic and peak systolic pressure were monitored during the KH perfusion, the rate pressure product was calculated and coronary flow was measured throughout the protocol. Two 4 min spectra were acquired. The perfusion buffer was then switched to LKH and five more spectra were acquired. Three or four function and flow measurements were taken. All flow to the heart was stopped and there was a 28 min period of ischemia during which seven spectra were collected. The time course and degree of contracture that developed during ischemia was measured. Following the ischemic period, the heart was reperfused with KH for 20 min, five spectra were acquired and the heart function was monitored for recovery. Four control hearts were perfused only with KH and subjected to the same perfusion, ischemia and reperfusion protocol. All spectra were analyzed using NMR1 on a Sun 3/160C Workstation and were quantified by comparison against the absolute integral of the MPA external standard.

5.3 Bench Experiments

In order to separate lithium effects on the heart from low sodium effects, bench experiments were conducted on a perfusion apparatus identical to the one used in the NMR studies. Hearts were perfused as described in the general methods with KH for 20 min while myocardial function and flow were monitored. The hearts were then paced at the slower heart rate observed in previous function studies with lithium perfusion and the buffer was changed to one containing 78 mM sodium and 78 mM choline for 10 min. The same protocol was repeated using a KH buffer with normal sodium (145 mM) and an additional 50 mM LiCl or 50 mM choline.

5.4 Results

In switching from the KH to the LKH buffer, the heart rate decreased 24%, the end diastolic pressure remained constant while the peak systolic pressure increased 157%, giving

an increase in developed pressure of 174% which gave a 105% increase in the rate pressure product (Fig. 5.2). At the same time the coronary flow increased by 40% (Table 5.1) The data are the pooled values from the 4 hearts perfused with LKH for 48 min and the four hearts from

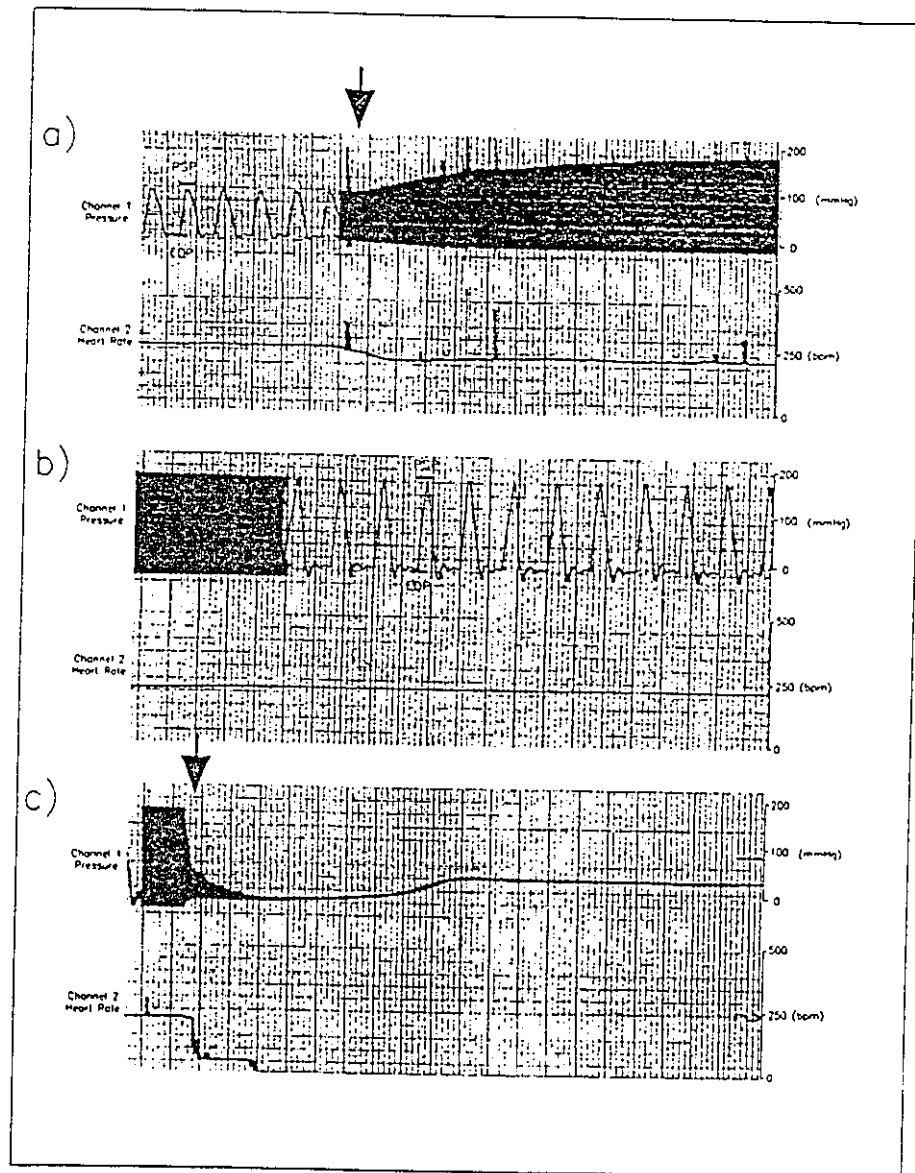


Fig. 5.2: Myocardial pressure and heart rate during a) perfusion with Krebs Henseleit (KH) which was then switched (arrow) for lithium KH (LKH) b) LKH for 20 min c) Total global ischemia (arrow) for 28 min. End diastolic pressure (EDP) and peak systolic pressure (PSP) are indicated by bars in a) and b).

the ischemia/reperfusion protocol and all the parameters measured with the exception of the EDP and coronary flow, were significantly different between control and LKH perfused hearts ($p < 0.001$) using analysis of variance. The EDP was constant and the coronary flows between groups were not significantly different, having a $p = 0.06$.

Table 5.1: Effect of LKH perfusion on myocardial function and flow

	KH	LKH	% Change
Heart Rate (beats/min)	326 ± 35	246 ± 33	-24
End Diastolic Pressure (mmHg)	7 ± 4	7 ± 3	none
Peak Systolic Pressure (mmHg)	79 ± 16	203 ± 55	+157
Developed Pressure (mmHg)	71 ± 16	195 ± 55	+174
Rate Pressure Product (10^3 mmHg/min)	23 ± 5	47 ± 10	+105
Coronary Flow (ml/min)	20 ± 7	28 ± 8	+40

Buffer: 78 mM Li^+ + 78 mM Na^+ Data represent the means \pm SD., $n = 8$

In switching from KH to KH choline buffer, the developed pressure in the hearts increased by 92%. In both these buffers the sodium concentration gradient across the sarcolemma changed from 6.3 ($\text{Na}_o:\text{Na}_i$, 144 mM:23 mM) to 3.4 ($\text{Na}_o:\text{Na}_i$, 78 mM:23 mM), but after 20 minutes perfusion with LKH buffer the sodium gradient had increased to 5.6 ($\text{Na}_o:\text{Na}_i$, 78 mM:14 mM) as intracellular sodium was depleted (see Table 4.2). Perfusion with KH containing an additional 50 mM lithium caused a 25% decrease in heart rate but had no effect on developed pressure. To determine if the 25% decrease in heart rate was due to the higher osmolality of the buffer, hearts were perfused with KH containing an additional 50 mM choline and a reduction in heart rate was observed (47%) with no effect on developed pressure. The rate pressure product of the control hearts during reperfusion was 0-4% of pre-ischemic values while the lithium perfused hearts showed a much better recovery with rate pressure products that were 18-35% of pre-ischemic values.

In the series of control experiments in which hearts were perfused with LKH for a 48 min perfusion period, the PCr and ATP peak areas varied by less than 8%. The Pi varied by ~16% because the peak was small and broad making it difficult to fit.

In the ischemia and reperfusion protocol, the effects of LKH and KH perfusion on the levels of PCr, ATP, Pi and pH, over the entire protocol, were assessed by a split-plot design analysis of variance, the results of which are summarized in the table 5.2. These results indicated that further statistical tests such as a two-way analysis of variance with repeated measures for separate sub-sections of the protocol, were required for PCr, ATP and pH since there was a significant ($p < 0.05$) interaction between the perfusion buffer effects and the protocol effects.

Table 5.2 : Statistical results of a split plot analysis of variance and covariance with repeated measures on steady state levels of PCr, ATP, Pi and pH of LKH perfused hearts

	PCr		ATP		Pi		pH	
	F-test	p value	F-test	p value	F-test	p value	F-test	p value
Buffer Effect	5.70	0.03	0.15	0.71	0.41	0.53	11.9	0.003
Protocol Effect	216	0.0001	152.61	0.0001	43.13	0.0001	65	0.0001
Interaction	26	0.0001	4.40	0.028	2.82	0.09	4.45	0.03

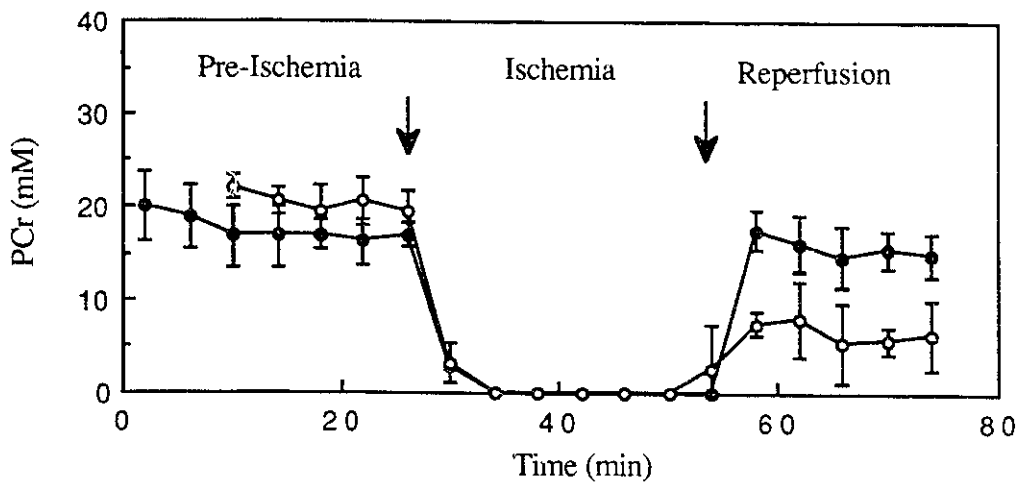


Fig. 5.3 Change in PCr during pre-ischemia, 28 min ischemia and reperfusion with LKH (●) and KH (○) buffers. Data are presented as the means \pm SD.

In the ischemia and reperfusion protocol, the PCr peak area remained stable upon switching to the LKH buffer. The PCr of the lithium perfused hearts was significantly different from the control hearts during the pre-ischemic period ($p = 0.039$) and during reperfusion ($p = 0.002$) when the LKH perfused hearts PCr recovered at a faster rate and to a 44% higher level than control hearts (Fig.5.3). LKH perfused hearts recovered to 94% of their pre-ischemic PCr levels, while controls hearts recovered 32%.

The ATP concentrations in the control and lithium perfused hearts were not significantly different during the pre-ischemia ($p = 0.06$) and reperfusion ($p = 0.09$) periods of the protocol, but there was a significant difference ($p = 0.03$) between groups and interaction between buffer and time course ($p = 0.03$) during ischemia (Fig. 5.4).

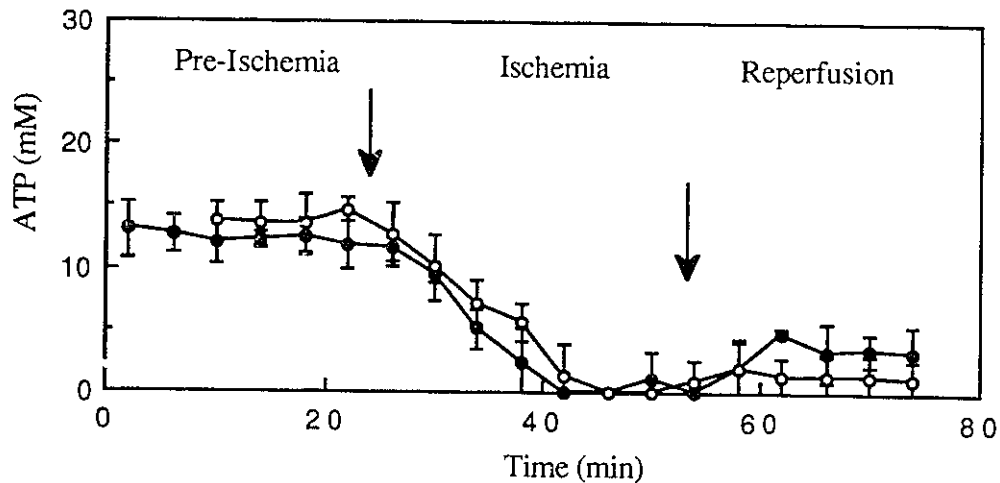


Fig. 5.4: Change in ATP during pre-ischemia, 28 min ischemia and reperfusion with LKH (●) and KH (○) buffers. Data are presented as the means \pm SD.

The inorganic phosphate peaks were broad and difficult to quantify in both the control and LKH perfused hearts, therefore the standard deviations between hearts were larger for Pi than for the other phosphorus peaks. The Pi in the control and LKH groups was the same throughout the perfusion protocol.

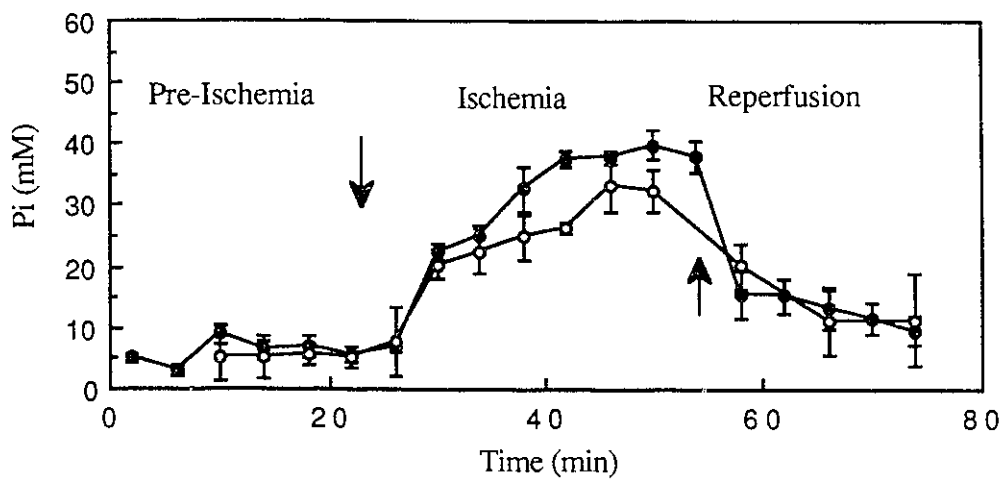


Fig. 5.5: Change in Pi during pre-ischemia, 28 min ischemia and reperfusion with LKH (●) and KH (○) buffers. Data are presented as the means \pm SD.

The intracellular pH, monitored by the chemical shift of the Pi peak, was the same for both groups of hearts during the pre-ischemic and reperfusion periods, but was significantly lower ($p = 0.0001$) in the control hearts during ischemia (Fig 5.6).

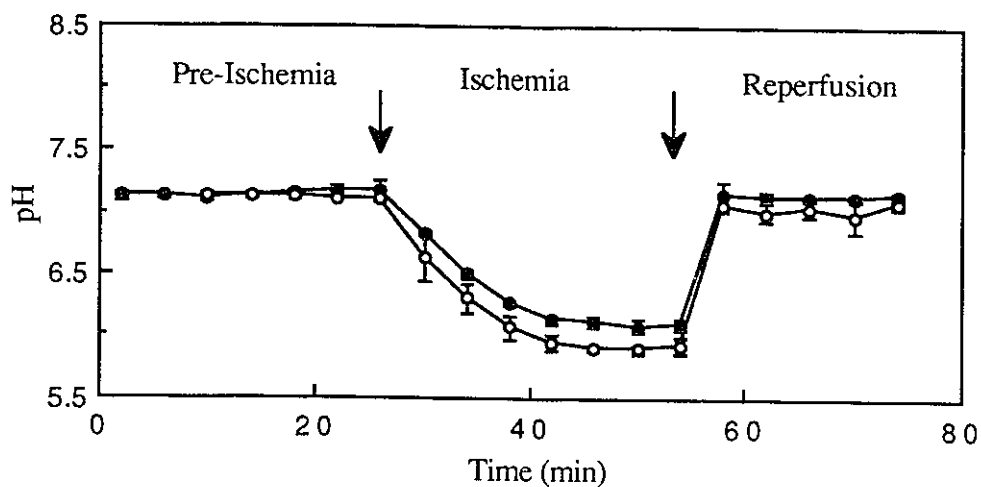


Fig. 5.6: Change in pH during pre-ischemia, 28 min ischemia and reperfusion with LKH (●) and KH (○) buffers. Data are presented as the means \pm SD.

5.5 Discussion

Perfusion with a low-sodium, lithium-containing buffer has a marked effect on myocardial contractile function, but has little effect on the overall concentrations of the high energy phosphorus metabolites. It is likely that the turnover rate of PCr and ATP increased when the increase in function occurred and this would be interesting to investigate in future experiments either with thermister (to measure the heat given off during the increase in function) or using the NMR technique of saturation transfer (to measure the flux of high energy phosphate metabolite movements across the sarcolemma). There were no significant differences in PCr, ATP or Pi between control and LKH perfused hearts, both during a 48 min perfusion protocol and during the ischemia-reperfusion protocol. The results of the 48 min perfusion with LKH indicate the functional and metabolic stability of the preparation. The

contractile function effects observed during the pre-ischemia perfusion period were not due to a direct effect of lithium on the heart but were due to the initial reduction in the transsarcolemmal sodium gradient from 6.3 to 3.4, which decreased $\text{Na}^+/\text{Ca}^{2+}$ exchange and increased sarcoplasmic reticular calcium uptake and release. This was demonstrated by the experiments in which choline was used as a sodium substitute. Choline is not as good as lithium as a sodium substitute since it cannot pass through the fast sodium channels. The hearts had to be paced so the stimulation was not exactly the same as with LKH perfused hearts, thus similar qualitative changes in function were observed but the extent of increase in systolic pressure was not as great as with lithium perfusion. This conclusion was confirmed by perfusing hearts with KH buffer containing an extra 50 mM lithium and no increase in function was observed. Lithium has been shown to effect contractility and calcium release during alpha adrenoceptor stimulation through inhibition of the inositol-1-phosphatase leading to an increase in inositol-1-phosphate (Mantelli *et al*, 1988). It is highly unlikely that such an upregulation of this system could occur instantaneously upon the LKH buffer reaching the heart. A reduction in the sodium gradient resulted in the modulation of $\text{Na}^+/\text{Ca}^{2+}$ exchange, which is reversible, the direction depending on the sodium and calcium electrochemical gradients and on the transmembrane potential (Bers, 1990). Under normal conditions, the exchanger transports sodium in and calcium out of the cell. It has been postulated that this exchange reverses at the peak of the cardiac cycle (Noble, 1984) and contributes to the decrease in intracellular calcium concentration following contraction. A reduction in the sodium gradient leads to an overall increase in intracellular calcium content (Sheu and Fozzard, 1982). The increased intracellular calcium is sequestered in the sarcoplasmic reticulum and a greater amount of calcium is released upon each cycle of excitation and contraction. This causes greater activation of the contractile proteins and an increase in the developed force during contraction.

The characteristics of the inotropic response of the heart to perfusion with low sodium buffer depends on the amount of sodium replaced in the solution (Kolar *et al.*, 1990) and

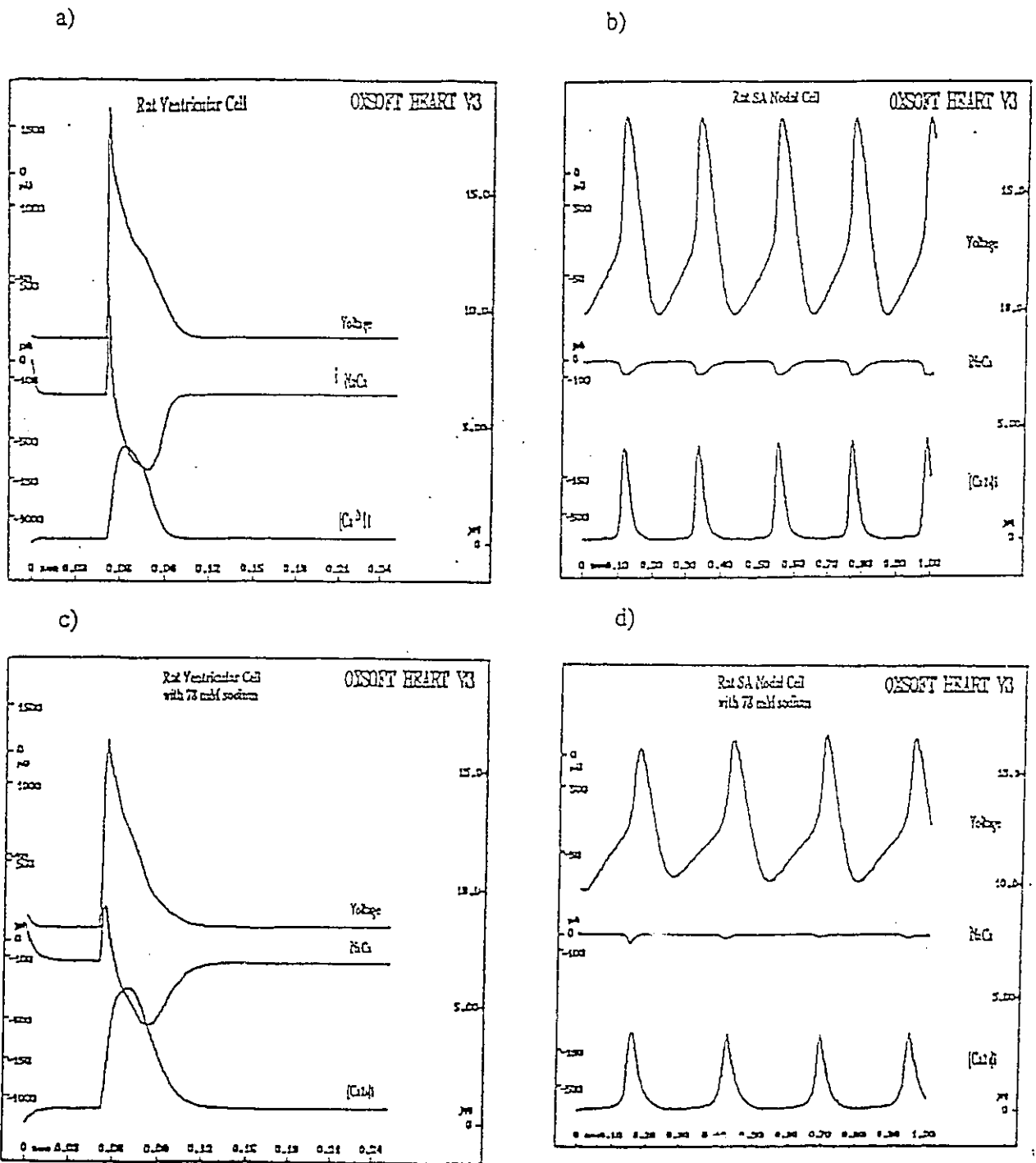


Fig. 5.6 a) Normal ventricular cells b) Normal sinoatrial node cells c) Ventricular cells perfused with 78 mM extracellular sodium d) Sinoatrial node cells perfused with 78 mM extracellular sodium

thereby the relative changes in the transmembrane sodium gradient. In the cases where the sodium concentration has been reduced to zero, the hearts exhibit an initial increase in contractility followed by a depolarization of the resting membrane potential and a rise in the resting tension or diastolic pressure (Lüttgau and Niedergerke, 1958; Chapman *et al.*, 1974, 1983; Langer and Nudd, 1984). These effects are due to an excessive rise in intracellular calcium with which the heart is unable to cope. Less drastic reductions in the sodium gradient (50-70%) result in enhanced contractility without a rise in diastolic pressure (Lullmann *et al.*, 1990; Sheu and Fozzard, 1982). The heart is able to sequester and release the extra intracellular calcium without compromising excitability or function. A computer model that simulates the ion fluxes in the ventricular and sinus node cells over the course of a normal wave of excitation-contraction in the heart (Dr. D. Noble, The University of Oxford, computer program OXSOFTE HEART) predicted the effects depicted above (Fig.5.7 a-d) when the heart was perfused with buffer containing 78 mM sodium. When the value of 78 mM was entered for the extracellular sodium concentration, the computer model predicted that there would be a 22% reduction in the heart rate and the amplitude of the action potential. As well, an increase in the inward calcium current and a decrease in the $\text{Na}^+/\text{Ca}^{2+}$ exchanger current (i_{NaCa}) were predicted. These predictions fit well with our results. We observed the 22% decrease in heart rate and a large increase in developed pressure, due to the overall increase in intracellular calcium.

In summary, the positive inotropic effect on myocardial function observed when perfusing with low sodium buffer (78 mM) does not affect the steady state concentrations of the myocardial high energy phosphate metabolites and is caused by an increase in the intracellular calcium released during each cycle of excitation and contraction.

CHAPTER SIX

CHARACTERIZATION OF TRANSSARCOLEMMAL LITHIUM TRANSPORT MECHANISMS

6.1 Introduction

6.2 Methods

6.3 Results

6.4 Discussion

6.1 Introduction

Sodium crosses the sarcolemma into myocardial cells, driven by its electrochemical gradient, through the voltage-gated fast sodium channels, by $\text{Na}^+/\text{Ca}^{++}$ exchange and by Na^+/H^+ exchange. It is pumped out of the cell by the energy dependent sodium pump (Fig. 1.1). Lithium crosses the sarcolemma into cells via the fast sodium channels (Carmeliet, 1964) and the Na^+/H^+ exchanger (Mahnensmith and Aronson, 1985), but cannot replace sodium in the Na^+ pump (Beaugé, 1975) or the $\text{Na}^+/\text{Ca}^{++}$ exchanger (Ponce-Hornos and Langer, 1980). In the following experiments, we determined the relative contributions of movement through the fast sodium channel and the Na^+/H^+ exchanger to the uptake of lithium in the perfused rat heart during control and ischemia protocols by inhibiting the Na^+/H^+ exchanger with amiloride (Piwnica-Worms *et al.*, 1985; Mahnensmith and Aronson, 1985; Kim and Smith, 1985). Amiloride is a pyrazinoylguanidine compound that has inhibitory effects on a number of ion transporters as well as its effects on the Na^+/H^+ exchanger. The IC_{50} of amiloride for inhibition of the Na^+ pump is 3 mM and for the $\text{Na}^+/\text{Ca}^{2+}$ exchanger it is 1 mM. The IC_{50} for inhibition of sodium flux through the voltage gated fast sodium channel is 0.6 mM, but it is unknown whether or not alterations in the extracellular sodium concentration affect the potency of amiloride inhibition of this channel (Kleyman and Cragoe, 1988). Amiloride has a greater affinity for the Na^+/H^+ exchanger ($\text{IC}_{50} = 30 \mu\text{M}$) than most of the other sodium transport processes and it was first used to inhibit this exchanger in 1976 by Johnson *et al.* A concentration of 1 mM was used in these experiments to ensure complete inhibition of the Na^+/H^+ exchanger while providing minimal inhibition of other sodium transport mechanisms. In further experiments, we inhibited the sodium pump with ouabain (Glynn, 1964; Lee and Klaus, 1971; Akera and Brody, 1978) and perfused the hearts with LKH buffer containing equal concentrations (78 mM) of sodium and lithium to determine whether the rates of uptake

of the two cations (Na^+ and Li^+) were similar. These studies involved the use of both ^{23}Na and ^7Li NMR spectroscopy.

6.2 Methods

6.2.1 Amiloride and Li^+/H^+ exchange

Rat hearts were perfused as described in the General Methods, with KH for 10 min to ensure that myocardial function and flow were normal when the perfusion buffer was changed to a KH buffer containing 1 mM amiloride to inhibit Na^+/H^+ exchange. After 10 min the buffer was then changed to LKHS containing 1 mM amiloride to wash lithium into the myocardial cells while inhibiting Na^+/H^+ exchange. The heart was surrounded by a KHS bath flowing at 35 ml/min, as described in the General Methods. Seven fully relaxed ^7Li NMR spectra were acquired with $\text{NS} = 4$ and $\text{RD} = 45$ s, providing a time resolution of 3 min and a total wash-in time of 23 min. Following wash-in, the LKHS buffer was switched off and the hearts were flushed immediately with a 0.35 M sucrose and 5 mM histidine solution at 5°C to remove perfusion buffer from the extracellular spaces. The KHS bath was flushed out (35 ml/min for 1 min) to remove any lithium that had been washed from the extracellular space and a final ^7Li NMR spectrum (intracellular lithium) was acquired before the hearts were freeze-clamped for ICP-AES analysis.

To determine the effects of amiloride during ischemia, the above protocol was followed, but 28 min ischemia was imposed after 20 min lithium wash-in with amiloride. During ischemia, 9 fully-relaxed ^7Li NMR spectra were acquired before the heart was flushed with the sucrose and histidine solution and the final intracellular lithium spectrum acquired. These hearts were freeze-clamped and analyzed by ICP-AES. Both of the above protocols

were repeated in a series of bench experiments and the hearts were extracted and lithium levels were determined using ICP-AES, to confirm the findings of the NMR experiments.

The NMR spectra from these experiments had low signal to noise, so they were plotted on high quality paper and the peak areas representing the reference solution and the intra- and extracellular lithium pools were cut and weighed in order to assess changes in sodium and lithium concentrations during the protocol. Statistical analyses were carried out using analysis of variance.

6.2.2 Ouabain and Na⁺ Pump Activity

Rat hearts were perfused with KH to establish normal cardiac function. After 10 min the perfusion buffer was changed to a modified LKH containing 0.1 mM ouabain and zero potassium to inhibit the Na⁺ pump. The hearts were surrounded by a mannitol bath containing shift reagent to remove from around the heart any sodium or lithium signals arising from the perfusate in the bath. A 2 min ²³Na NMR spectrum was acquired with NS = 480, RD = 0.09 s and PW = 30 μs. A 3 min ⁷Li NMR spectrum was acquired, followed by three ²³Na NMR spectra and one more ⁷Li NMR spectrum before the hearts were flushed with the cold sucrose and histidine solution. Final ²³Na and ⁷Li NMR spectra were acquired and the hearts were freeze-clamped and analyzed by ICP-AES. This gave a perfusion time of 20 min. A similar ouabain, zero potassium perfusion protocol was repeated in a series of bench experiments. The hearts were freeze-clamped at the end of the protocol and analyzed by ICP-AES.

To estimate normal intracellular sodium concentrations, hearts (n = 3) were perfused with KH in the shifted mannitol bath for 10 min, a ²³Na NMR spectrum was acquired and the hearts were washed out with the cold sucrose and histidine solution and another ²³Na NMR spectrum was acquired before the hearts were freeze-clamped and analyzed by ICP-AES.

The NMR data from these experiments were analyzed using the NMR1 software on a Sun 3/160C workstation. Intracellular concentrations were calculated using an external standard containing 7.0 μmoles of lithium and 8.2 μmoles of sodium.

6.3 Results

6.3.1 Amiloride and Li^+/H^+ exchange

Intracellular lithium reached a concentration of 47 mM in hearts ($n = 3$) perfused with LKH containing 1 mM amiloride which was not significantly different ($p > 0.05$) from the concentration of 55 mM in control hearts ($n = 3$) (Table 6.1). However, amiloride completely prevented the rise in intracellular lithium during ischemia, in marked contrast to control hearts in which intracellular lithium concentration was 78 mM at the end of the 28 min ischemia (Table 6.1). Table 6.1 also shows the close agreement between the lithium uptake measured using ^7Li NMR spectroscopy and ICP-AES.

Table 6.1 Effect of 1 mM amiloride on lithium uptake during perfusion and ischemia (mM)

Buffer	Pre-Ischemia		Ischemia	
	NMR	ICP-AES	NMR	ICP-AES
*LKH	55 ± 7	50 ± 2	78 ± 11	79 ± 12
LKH with Amiloride	47 ± 4	40 ± 4	47 ± 9	34 ± 6

Data presented are the means \pm SD ($n = 3$) * These means are from Table 4.1

In hearts perfused with LKH buffer, the $t_{1/2}$ to reach maximum contracture during ischemia was 13 ± 5 min and the maximum contracture pressure during ischemia was 30 ± 9 mmHg. When amiloride was added to the LKH buffer, the $t_{1/2}$ was 17 ± 2 min and the maximum contracture pressure was 15 ± 4 mmHg. The decrease in the maximum contracture pressure was significant ($p < 0.005$) when tested using a one-way analysis of variance.

6.3.2 Ouabain and Na^+ Pump Activity

Normal intracellular sodium in the perfused rat heart was estimated to be 27 ± 3 mM using ^{23}Na NMR spectroscopy and 23 ± 3 mM using ICP-AES. Rat hearts showed an immediate increase in rate pressure product (40%) on changing to the LKH with zero potassium and 0.1 mM ouabain. After approximately 4 min perfusion, the hearts ceased to beat as the sodium pump was inhibited and intracellular sodium concentrations rose.

^{23}Na NMR spectra from these hearts consisted of a large shifted extracellular sodium peak and a smaller unshifted intracellular sodium peak (Fig. 6.1). After the extracellular space had been washed out, a small peak representing sodium remaining in the bath and extracellular spaces was observed and the intracellular sodium resonance was clearly defined, being of comparable size to the sodium peak from the external reference (Fig. 6.1).

The ^7Li NMR spectra acquired immediately after the ^{23}Na NMR spectra showed a large shifted extracellular lithium peak and the unshifted intracellular peak appeared as a shoulder on the right side of the extracellular peak. Following washout of the extracellular space, the intracellular resonance became sharper, facilitating quantification (Fig. 6.2).

After 20 min perfusion with LKH buffer containing zero potassium and ouabain, the intracellular sodium reached a concentration of 39 mM, while the intracellular lithium concentration was 61 mM (Table 6.2). Again, as shown in Table 6.2, there was close agreement between the NMR and ICP-AES calculated values.

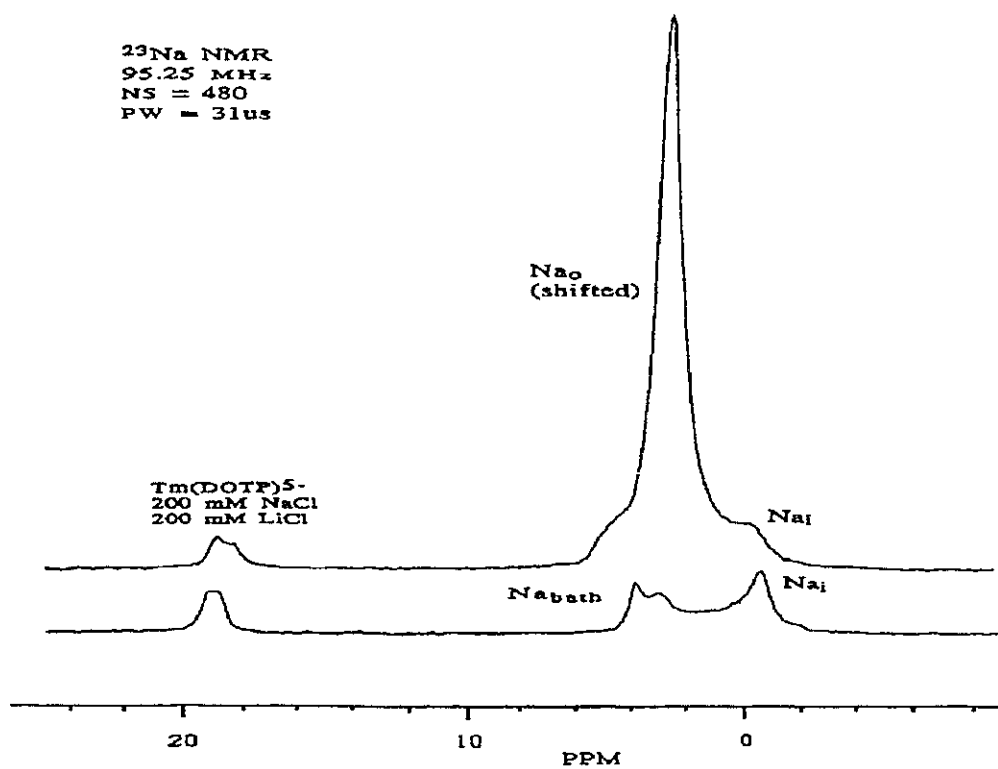


Fig. 6.1 Top trace: ^{23}Na NMR spectrum from a rat heart perfused for 20 min with LKHS buffer containing ouabain and zero potassium. Bottom trace: ^{23}Na NMR spectrum of the same heart after the extracellular space had been washed out.

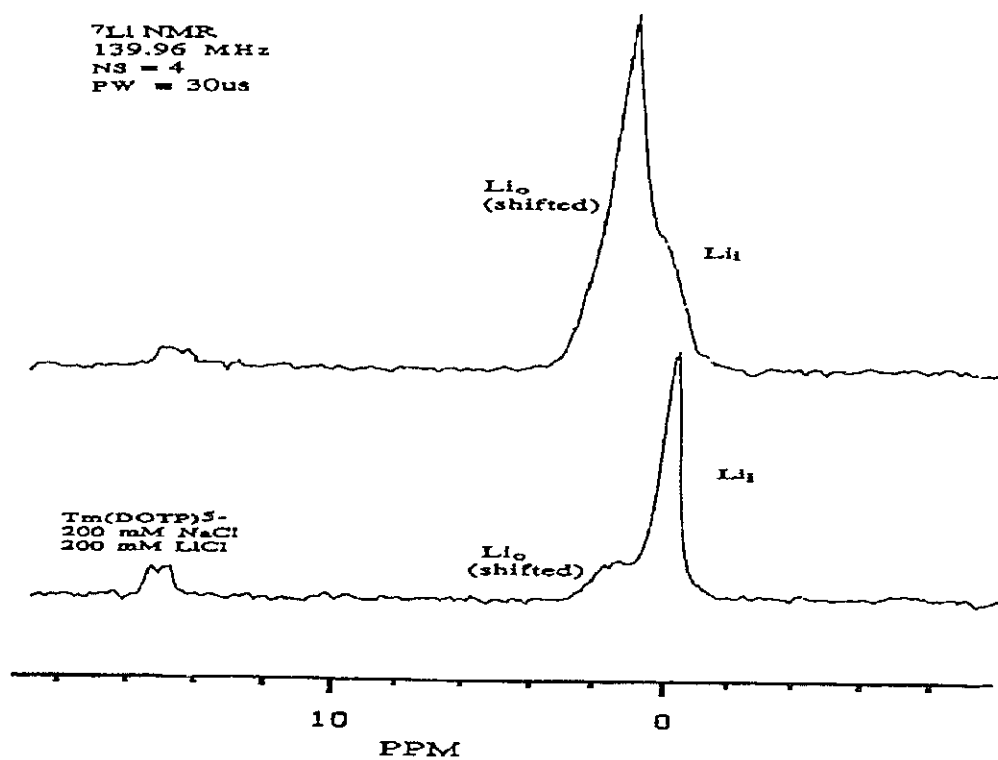


Fig. 6.2 Top trace: ⁷Li NMR spectra from a rat heart perfused for 20 min with LKHS buffer containing ouabain and zero potassium. Bottom trace: ⁷Li NMR spectra of the same heart after the extracellular space had been washed out.

Table 6.2 Intracellular Lithium and Sodium Concentrations After 20 min Perfusion with LKH Containing Ouabain and Zero Potassium

	NMR	ICP-AES
[Na ⁺] _i	39 ± 5	42 ± 4
[Li ⁺] _i	61 ± 9	61 ± 7

Data presented are the means ± SD (n = 5)

Intracellular sodium, potassium and lithium concentrations in hearts perfused for 20 min with KH buffer, LKH buffer and LKH buffer containing zero potassium and 0.1 mM ouabain were measured using ICP-AES and are shown in Table 6.3. In switching from KH to LKH buffer the intracellular sodium decreased by 50% and the potassium decreased by 35% as lithium moved into the myocytes. When the sodium pump was blocked and the hearts were perfused with LKH, intracellular sodium increased 3-fold, while the potassium decreased by 50% as further increases in the intracellular lithium occurred. The difference between the final intracellular lithium concentration with and without sodium pump inhibition was significant ($p < 0.05$) using a one-way analysis of variance.

Table 6.3 Intracellular Cation Concentrations After 20 min Perfusion with Various Buffers
Measured Using ICP-AES

	Buffer		
	KH (n = 3)	*LKH (n = 4)	LKH + Ouabain, no K ⁺ (n = 5)
[Na ⁺] _i	23 ± 3	14 ± 2	†42 ± 4
[Li ⁺] _i	0	50 ± 2	†61 ± 7
[K ⁺] _i	87 ± 5	57 ± 6	28 ± 3

Data represent the means ± SD * These values are from Table 4.2 †These values are from Table 6.2

6.4 Discussion

Cell damage following a period of ischemia is thought to be due to a large increase in intracellular calcium during reperfusion of the myocardium (Shen and Jennings, 1972; Poole-Wilson *et al.*, 1984; Nayler and Elz, 1986). Reversal of Na⁺/Ca²⁺ exchange is a likely route by which this influx of calcium occurs (Murphy *et al.*, 1991). During ischemia, there is an increase in intracellular proton concentration due to anaerobic glycolysis, which stimulates Na⁺/H⁺ exchange leading to an overall increase in intracellular sodium. The Na⁺/H⁺ exchange inhibitor, amiloride, attenuated the rise in intracellular sodium during ischemia, but had no effect during control perfusion (Murphy *et al.*, 1991). When we perfused hearts with LKH buffer in the presence of amiloride, we observed similar results in that amiloride had no effect on lithium uptake during the pre-ischemic perfusion period, whereas it completely abolished lithium uptake during ischemia. These results apparently contradict the possibility raised in Chapter 4 of the existence of Na⁺/Li⁺ and K⁺/Li⁺ exchanges since lithium uptake during

ischemia was completely abolished in the presence of amiloride. It may be that these exchangers are inhibited by amiloride, particularly Na^+/Li^+ exchange since amiloride inhibits most sodium transport mechanisms but it has not been shown to affect potassium transport mechanisms. If this was the case, then lithium uptake in the pre-ischemic heart should have been inhibited but we did not find it to be significantly reduced. Murphy *et al.* (1991) also noted that amiloride delayed the increase in resting tension that occurred during ischemia. They found that the $t_{1/2}$ to reach peak contracture occurred after ~ 8 min ischemia in control hearts and ~ 10 min in the amiloride treated hearts. This effect correlated with the rise in intracellular sodium during ischemia, which delayed the small rise in intracellular calcium that occurred in control hearts during ischemia and which is postulated to be responsible for ischemia-induced contracture. Our hearts were doubly protected against contracture during ischemia because perfusion with low sodium buffer resulted in a 50% lower intracellular sodium and an increase in the $t_{1/2}$ to reach maximal contracture during ischemia, from ~ 8 min to ~ 16 min. The peak contracture pressure in these hearts was 50% of that reached by normal hearts during ischemia. The addition of amiloride to the LKH buffer did not affect the $t_{1/2}$ during ischemia but it did cause a 50% decrease in the peak contracture pressure from that of the LKH perfused hearts.

The cardiac glycoside, ouabain, is a known inhibitor of the sodium pump (Glynn, 1964; Akera and Brody, 1978). During ouabain and/or zero external potassium perfusion, the sodium pump was inhibited and intracellular sodium increased by 170% (Lotan *et al.*, 1991). This increase in intracellular sodium resulted in a calcium influx via reversed $\text{Na}^+/\text{Ca}^{2+}$ exchange, which caused an increase in cardiac contractility (Barry *et al.*, 1985). In the case of perfusion with low sodium buffer, normal $\text{Na}^+/\text{Ca}^{2+}$ exchange decreased because the transsarcolemmal sodium gradient was reduced, resulting in an increase in intracellular calcium and cardiac developed pressure. We investigated the effects of simultaneously lowering the sodium gradient and blocking the sodium pump on the intracellular concentrations of lithium, sodium and potassium. Lithium entered the heart through the fast sodium channels and the

Na^+/H^+ exchanger and accumulated in the cell, not being actively extruded. If the sodium pump were blocked and the sodium gradient reduced, cellular influx of sodium would occur via the fast sodium channels and Na^+/H^+ exchange and should be similar to cellular lithium uptake. We found a slightly greater increase in lithium uptake during sodium pump inhibition than during normal LKH perfusion, possibly reflecting an increase in the affinity of the fast sodium channels and the Na^+/H^+ exchanger for lithium. Intracellular sodium did not increase to the same extent as intracellular lithium during sodium pump inhibition. Perfusion with LKH buffer resulted in a 40% decrease in intracellular sodium. When the sodium pump was inhibited and the heart was perfused with LKH, the intracellular sodium rose 200% from its LKH alone value which agrees with the 170% increase in intracellular sodium observed by Lotan *et al.* (1991) and it rose 83% from its normal, control value. The intracellular sodium moved towards its equilibrium value, as did the lithium, but not as quickly, probably due to reversed $\text{Na}^+/\text{Ca}^{++}$ exchange which offset the effects of sodium pump inhibition. Inhibition of the sodium pump also caused a 68% loss of potassium from the cells, which moved out as lithium and sodium moved in.

In summary, we found that increases in sodium and lithium during ischemia occur via a Na^+/H^+ and Li^+/H^+ exchange mechanisms. During perfusion with low sodium buffer, intracellular sodium increased to a similar extent during sodium pump inhibition as it did in hearts perfused with normal (145 mM sodium) buffer. The inhibition of the sodium pump in hearts perfused with low sodium buffer caused an ~60% loss of potassium from the cells which was replaced by sodium and lithium.

CHAPTER SEVEN

GENERAL CONCLUSIONS

Intracellular sodium concentrations increase ~4-fold during 30 min total, global ischemia in the isolated rat heart. It is thought that the increase in intracellular sodium is a consequence of inward transsarcolemmal sodium movement down its electrochemical gradient, while sodium efflux is limited by inhibition of the sodium pump secondary to ATP depletion and accumulation of ATP hydrolysis products. The decreased transsarcolemmal sodium gradient may lead to reversed $\text{Na}^+/\text{Ca}^{++}$ exchange and therefore calcium influx during ischemia and the early stages of reperfusion, this calcium causing irreversible ischemic damage to the myocardial cells.

^{23}Na NMR spectroscopy can be used to measure intracellular sodium, but the intra- and extracellular signals are often poorly resolved. ^7Li NMR spectroscopy was used to characterize transsarcolemmal sodium movements because lithium is a biological congener for sodium with twice the NMR sensitivity as sodium. In order to perform these studies accurately, the relaxation behavior of lithium in the myocardium and perfusion buffers was determined. The T_1 and T_2 for lithium in Krebs Henseleit buffer were 25 s and 19 s, respectively. The lithium-perfused heart has a single lithium NMR peak which has a T_1 of 6.9 s and a biexponential T_2 with a fast component of 0.17 s and a slow component of 0.85 s. When the shift reagent, DyTTHA^{3-} was present in the perfusion buffer, the intra- and extracellular lithium peaks could be distinguished. Intracellular lithium was found to have a relatively long T_1 of 9 s and a biexponential T_2 with a fast component of 0.04 s and a slow component of 1.12 s. The addition of DyTTHA^{3-} considerably shortened the relaxation times for lithium in buffer such that the T_1 was 0.65 s and the T_2 was 0.49 s.

^{31}P NMR was used to show that although perfusion of the heart with a low-sodium, lithium-containing buffer had positive inotropic effect on myocardial function, it did not affect steady state levels of myocardial high energy metabolites. We showed that the increase in systolic pressure was due to the reduction in the sodium electrochemical gradient which

decreased $\text{Na}^+/\text{Ca}^{++}$ exchange, thereby causing an increase in the intracellular calcium during each cycle of excitation and contraction.

In examining the kinetics of lithium movements across the sarcolemma, we found that the influx of lithium had a rate constant (k_i) of 0.068 min^{-1} , a $t_{1/2}$ of 10.3 min and an initial rate of increase of 5.27 mM/min and the lithium efflux had a k_e of 0.062 min^{-1} , a $t_{1/2}$ of 11.2 min and an initial rate of 4.83 mM/min. Lithium equilibrated in the heart with equal concentrations on either side of the sarcolemma, not according to its electrochemical equilibrium. When the modes of sodium flux across the cell membrane were limited by ouabain inhibition of the sodium pump, they more closely resembled those of lithium entry. We used ^{23}Na and ^7Li NMR spectroscopy to examine the uptake of sodium and lithium during sodium pump inhibition and found that the extent of the intracellular sodium increase was less than the extent of intracellular lithium increase, possibly because sodium efflux continued to occur via reversed $\text{Na}^+/\text{Ca}^{++}$ exchange. We found that lithium increased in a linear fashion during ischemia at a rate of 1.34 mM/min, which is similar to the increase in sodium. The uptake of lithium during myocardial ischemia was completely blocked by the Na^+/H^+ exchange inhibitor, amiloride. Thus, it can be concluded from these studies that Na^+/H^+ exchange is the major transport mechanism for the increase in intracellular sodium during ischemia.

REFERENCES

- AKERA, T., BRODY, T.M. Myocardial membranes: Regulation and function of the sodium pump. *Ann Rev Physiol* 44, 375-388 (1982).
- AKERA, T., BRODY, T.M. The role of Na,K-ATPase in the inotropic action of digitalis. *Pharmacol Rev* 29, 187-200 (1978).
- ANDERSON, R.E., NEDELEC, J.F., MILLS, P.A., CLARKE, K. Changes in the transsarcolemmal sodium gradient during ischemia: A ³¹P and ²³Na NMR spectroscopy study of the isovolumic rat heart. *Circulation* 82, 759 (1990).
- ANDERSON, S.E., MURPHY, E., STEENBERGEN, C., LONDON, R.E., CALA, P.M. Na-H exchange in myocardium: effects of hypoxia and acidification on Na and Ca. *Am J Physiol* 259, C940-C948 (1990).
- BALSCHI, J.A., FRAZER, J.C., FETTERS, J.K., CLARKE, K., SPRINGER, C.S. Jr., SMITH, T.W., INGWALL, J.S. Shift reagent and ²³Na nuclear magnetic resonance discriminates between extra- and intracellular sodium pools in ischemic heart. *Circulation* 72, 355 (1985).
- BAKER, H.J., LINDSEY, J.R., WEISBROTH, S.H. *The laboratory rat*. Vol II. New York: Academic Press, pp 257-258 (1980).
- BARRY, W.H., HASIN, Y., SMITH, T.W. Sodium pump inhibition, enhanced calcium influx via sodium-calcium exchange and positive inotropic response in cultured heart cells. *Circ Res* 56, 231-241 (1985).
- BEAUGÉ, L. The interaction of lithium ions with the sodium-potassium pump in frog skeletal muscle. *J Physiol* 246, 397-420 (1975).

BERS, D.M., LEDERER, W.J., BERLIN, J.R. Intracellular Ca⁺ transients in rat cardiac myocytes: role of Na-Ca exchange in excitation-contraction coupling. *Am J Physiol* 258, C944-C954 (1990).

BHOJANI, I.H., CHAPMAN, R.A. The effects of bathing sodium ions upon the intracellular sodium activity in calcium-free media and the calcium paradox of isolated ferret ventricular muscle. *J Mol Cell Cardiol* 22, 507-522 (1990).

BURSTEIN, D., FOSSEL, E.T. Intracellular sodium and lithium NMR relaxation times in the perfused frog heart. *Mag Res Med* 4, 261-273 (1987).

BURSTEIN, D., FOSSEL, E.T. Nuclear magnetic resonance studies of intracellular ions in perfused frog heart. *Am J Physiol* 252, H1138-H1146 (1987).

CARMELIET, E.E. Influence of lithium ions on the transmembrane potential and cation content of cardiac cells. *J Gen Physiol* 47, 501-530 (1964).

CHAPMAN, R.A. A study of the contractures induced in frog atrial trabeculae by a reduction of the bathing sodium concentration. *J Physiol* 237, 295-313 (1974).

CHAPMAN, R.A. Control of cardiac contractility at the cellular level. *Am J Physiol* 245, H535-H552 (1983).

CHU, S.C., XU, Y., BALSCHI, J.A., SPRINGER, C.S. Jr. Bulk magnetic susceptibility shifts in NMR studies of compartmentalized samples: use of paramagnetic shift reagents. *Mag Reson Med* 13, 239-262 (1990).

CHU, S.C., PIKE, M.M., FOSSEL, E.T., SMITH, T.W., BALSCHI, J.A., SPRINGER, C.S. Jr. Aqueous shift reagents for high-resolution cationic nuclear magnetic resonance. III. Dy(TTHA)³⁻, Tm(TTHA)³⁻, and Tm(PPP)²⁷⁻. *J Magn Reson* 56, 33-47 (1984).

CLARKE, K, BALSCHI, JA, NEUBAUER, S, KLÉBER, AG, SPRINGER, CS Jr, SMITH, TW, INGWALL, JS Changes in the sarcolemmal pH gradient during ischemia and reperfusion: A ³¹P NMR study of the isolated rat heart. (Abstract) SMRM 43, 99 (1988).

CLARKE, K., NEDELEC, J-F, HUMPHREY, S.M., NEUBAUER, S., BALSCHI, JA , KLÉBER, A.G., SPRINGER, C.S., Jr., SMITH, T.W., INGWALL, J.S. Extracellular volume and transsarcolemmal proton movement during ischemia and reperfusion: A ³¹P NMR spectroscopy study of the isovolumic rat heart. NMR in Biomedicine , (in press) (1992).

CLARKE, K., O'CONNOR, A.J., WILLIS, R.J. Temporal relation between energy metabolism and myocardial function during ischemia and reperfusion. Am J Physiol 253, H412-H421 (1987).

DALBY, A.J., BRICKNELL, O.L., OPIE, L.H. Effect of glucose-insulin-potassium infusions on epicardial ECG changes and on myocardial metabolic changes after coronary artery ligation in dogs. Cardiovasc. Res 15, 588-598 (1981).

DORING, H.J., DEHNERT, H. *The isolated perfused heart according to Langendorff*. March, West Germany: Biomesstechnik-Verlag pp 1-100 (1988).

FOY, B.D., BURSTEIN, D. Interstitial sodium nuclear magnetic resonance relaxation times in perfused hearts. Biophys J 58, 127-134 (1990).

GLYNN, I.M. The action of cardiac glycosides on ion movements. Pharmacol Rev 16, 381-407 (1964).

GOW, I.F., ELLIS, D. Effect of lithium on the intracellular potassium concentration in sheep heart Purkinje fibres. Exper Physiol 75, 427-430 (1990).

GULLAPALLI, R.P., HAWK, R.M., KOMOROSKI, R.A. A ⁷Li study of visibility, spin relaxation and transport in normal human erythrocytes. Magn Res Med 20, 240-252 (1990).

- KEYNES, R.D., STEINHARDT, R.A., The components of the sodium efflux in frog muscle. *J. Physiol.* 198, 581-599 (1968).
- KEYNES, R.D., SWAN, R.C. The permeability of frog muscle fibres to lithium ions. *J Physiol* 147, 626-638 (1959).
- KIM, D., SMITH, T.W. Effects of thyroid hormone on sodium pump sites, sodium content and contractile responses to cardiac glycosides in cultured chick ventricular cells. *J Clin Invest* 74, 1481-1488 (1984).
- KIMURA, J., NOMA, A., IRISAWA, H. Na-Ca exchange in mammalian heart cells. *Nature* 319, 596-597 (1986).
- KLEYMAN, T.R., CRAGOE, E.J. Amiloride and its analogs as tools in the study of ion transport. *J Memb Biol* 105, 1-21 (1988).
- KOHLER, S.J., PERRY, S.B., STEWART, L.C., ATKINSON, D.E., CLARKE, K., INGWALL, J.S. Analysis of ²³Na NMR spectra from isolated perfused hearts. *Magn Reson Med* 18, 15-27 (1991).
- KOLAR, F., COLE, W.C., OSTADAL, B., DHALLA, N.S. Transient inotropic effects of low extracellular sodium in perfused rat heart. *Am J Physiol* 259, H712-H719 (1990).
- LANGER, G.A., NUDD, L.M. Calcium compartmentation in cardiac tissue culture: The effects of extracellular sodium depletion. *J Mol Cell Cardiol* 16, 1047-1057 (1984).
- LASZLO, P. The alkali metals. In: J.B. Lambert, F.G. Riddell (eds) *The multinuclear approach to NMR spectroscopy*, Dordrecht: Reidel Publishing Company pp. 261-296 (1983).
- LAZDUNSKI, M., FRELIN, C., VIGNE, P. The sodium/hydrogen exchange system in cardiac cells: Its biochemical and pharmacological properties and its role in regulating internal concentrations of sodium and internal pH. *J Mol Cell Cardiol* 17, 1029-1042 (1985).

LEE, C.O., FOZZARD, H.A., Activities of potassium and sodium ions in rabbit heart muscle. *J Gen Physiol* 65: 695-708 (1975).

LEE, K.S., KLAUS, W. The subcellular basis for the mechanism of ionotropic action of cardiac glycosides. *Pharmacol Rev* 23, 191-261 (1971).

LEHNINGER, A.L. Ca²⁺ transport by mitochondria and its possible role in the cardiac contraction-relaxation cycle. *Circ Res* 35(Suppl 3), 83-90 (1974).

LOTAN, C.S., MILLER, S.K., POHOST, G.M., ELGAVISH, G.A. Amiloride in ouabain-induced acidification, ionotropy and arrhythmia: ²³Na and ³¹P NMR in perfused hearts. *J Mol Cell Cardiol* 24, 243-257 (1992).

LULLMANN, H., RAVENS, U., STOCKEL, P. Changes of isolated cardiac muscle function in response to extracellular sodium reduction. *Pharm Toxic* 68, 35-45 (1991).

LÜTTGAU, H.C., NIEDERGERKE, R. The antagonism between Ca and Na ions on the frog's heart. *J Physiol* 143, 486-505 (1958).

MAHNENSMITH, R.L., ARONSON, P.S. The plasma membrane sodium-hydrogen exchanger and its role in physiological and pathophysiological processes. *Circ Res* 56, 773-788 (1985).

MALLOY, C.R., BUSTER, D.C., CASTRO, M.M.C., GERALDES, C.F.G., JEFFREY, F.M.H., SHERRY, A.D. Influence of global ischemia on intracellular sodium in the perfused rat heart. *Magn Reson Med* 15, 33-44 (1990).

MANTELLI, .L., CAPANNI, L., CORTI, V., BENNARDINI, F., MATUCCI, R., LEDDA, F. Influence of lithium on the positive inotropic effect of phenylephrine and isoprenaline in guinea-pig heart. *Eur J Pharm* 150, 123-129 (1988).

- MURPHY, E., PERLMAN, M., LONDON, R.E., STEENBERGEN, C. Amiloride delays the ischemia-induced rise in cytosolic free calcium. *Circ Res* 68, 1250-1258 (1991).
- NEDELEC, J.F., ANDERSON, R.E., ST.JEAN, M., CLARKE, K. Transmembrane lactate movement in the ischemic myocardium: ^1H , ^{23}Na and ^{31}P NMR spectroscopic studies of proton efflux mechanisms in the rat heart. (Abstract) SMRM 1, 842 (1992).
- NEELY, J.R., GROTYOHANN, L.W. Role of glycolytic products in damage to ischemic myocardium. Dissociation of adenosine triphosphate levels and recovery of function of reperfused ischemic hearts. *Circ Res* 55, 816-824 (1984).
- NIEDERGERKE, R., ORKAND, R.K. The dependence of the action potential of the frog's heart on the external and intracellular sodium concentration. *J Physiol* 184, 312-334 (1966).
- NOBLE, D. The surprising heart: A review of recent progress in cardiac electrophysiology. *J Physiol* 353, 1-50 (1984).
- OPIE, L., H. *The Heart: Physiology and Metabolism 2nd Edition* : New York: Raven Press pp. 1-500 (1991).
- PETTEGREW, J.W., POST, J.F.M., PANCHALINGAM, A., WITHERS, G., WOESSNER, D.E. ^7Li NMR study of normal human erythrocytes. *J Magn Reson* 71, 504-519 (1987).
- PETTEGREW, J.W., WOESSNER, D.E. ^{23}Na and ^7Li NMR studies of mammalian cells: Assessment of cation transport and cytoskeletal structure with application to manic depressive disease. In: J.W. Pettegrew (ed) *NMR: Principles and Applications to Biomedical Research*, New York: Springer-Verlag pp. 355-399 (1989).
- PIKE, M.M., FOSSEL, E.T., SMITH, T.W., SPRINGER, C.S. High-resolution ^{23}Na -NMR studies of human erythrocytes: use of aqueous shift reagents. *Am J Physiol* 246, C528-C536 (1984).

PIKE, M.M., FRAZER, J.C., DEDRICK, D.F., INGWALL, J.S., ALLEN, P.D., SPRINGER, C.S. Jr., SMITH, T.W. ^{23}Na and ^{39}K nuclear magnetic resonance studies of perfused rat hearts. Discrimination of intra- and extracellular ions using a shift reagent. *Biophys J* 48, 159-173 (1985).

PIWNICA-WORMS, D., JACOB, R., HORRES, C.R., LIEBERMAN, M. Na/H exchange in cultured chick cardiac cells, pH_i regulation. *J Gen Physiol* 85, 43-64 (1985).

POLIMENI, P., I. Measurement of myocardial electrolyte distributions. In: R.J. Linder (ed) *Techniques in the Life Sciences, P3/III: Cardiovascular Physiology* County Clare, Ireland: Elsevier Scientific Publishers Ireland Ltd., pp. 1-34 (1984).

PONCE-HORNOS, J.E., LANGER, G.A. Sodium-calcium exchange in mammalian myocardium: the effects of lithium. *J Mol Cell Cardiol* 12, 1367-1382 (1980).

POOLE-WILSON, P.A., HARDING, D.P., BOURDILLON, P.D.V., TONES, M.A. Calcium out of control. *J Mol Cell Cardiol* 16, 175-187 (1984).

POWELL, T., NOBLE, D. Calcium movements during each heart beat. *Mol Cell Biochem* 89, 103-108 (1989).

RAVENS, U., WETTWER, E. Modulation of sodium/calcium exchange: a hypothetical positive inotropic mechanism. *J Cardiovasc. Pharmacol.* 14, S30-S35 (1989).

SHEN, A.C., JENNINGS, R.B. Myocardial calcium and magnesium in acute ischaemic injury. *Am J Pathol* 67, 416-444 (1972).

SHEU, S-S, FOZZARD, H.A. Transmembrane Na^+ and Ca^{2+} electrochemical gradients in cardiac muscle and their relationship to force development. *J Gen Physiol* 80, 325-351 (1982).

SHINAR, H., NAVON, G. NMR studies of intracellular Na⁺ in red blood cells. *Biophys Chem* 20, 275-283 (1984).

SPRINGER, C.S., Jr., Measurement of metal cation compartmentalization in tissue by high-resolution metal cation NMR. *Ann Rev Biophys Biophys Chem* 16, 375-399 (1987).

SPRINGER, C.S., PIKE, M.M., BALSCHI, J.A., CHU, S.C., FRAZIER, J.C., INGWALL, J.S., SMITH, T.W. Use of shift reagents for nuclear magnetic resonance studies of the kinetics of ion transfer in cells and perfused hearts. *Circulation* 72, IV89-IV93 (1985).

STEIN, W.D., In: *Channels, Carriers and Pumps: An Introduction to Membrane Transport*, San Diego: Academic Press, pp. 73-123 (1990).

TANI, M., NEELY, J.R. Role of intracellular Na⁺ in Ca⁺ overload and depressed recovery of ventricular function of reperfused ischemic rat hearts. Possible involvement of H⁺-Na⁺ and Na⁺-Ca²⁺ exchange. *Circ Res* 65, 1045-1056 (1989).

TANI, M., NEELY, J.R. Intermittent perfusion of ischemic myocardium: possible mechanisms of protective effects on mechanical function in isolated rat heart. *Circulation*, 82, 536-548 (1990).

WOESSNER, D.E. Relaxation theory with applications to biological studies. In: J.W. Pettegrew (ed) *NMR: Principles and Applications to Biomedical Research*, New York: Springer-Verlag pp. 37-67 (1989).

YONEMURA, K., SATO, M. The resting membrane potential and cation movement in frog muscle fibres after exposure to lithium ions. *Japan J Physiol* 17, 678-697 (1967).

PUBLICATIONS

WALLEY, V.M., KEON, C.A., KHALILI, M., MOHER, D., CAMPAGNA, M., KEON, W.J. Ionescu-Shiley valve failure I: experience with 125 standard-profile explants The Annals of Thoracic Surgery 54 (1), 111-116 (1992).

WALLEY, V.M., KEON, C.A., KHALILI, M., MOHER, D., CAMPAGNA, M., KEON, W.J. Ionescu-Shiley valve failure II: experience with 25 low-profile explants The Annals of Thoracic Surgery 54 (1), 117-123 (1992).

WOLFSOHN, A.L., WALLEY, V.M., DAVIES, R.A., KEON, C.A., KHALILI, M., KEON, W.J. The University of Ottawa Heart Institute cardiac transplant program: the first 100 transplants. A pathologic study of the explanted hearts Modern Pathology 5 (2), 158-164 (1992).

ABSTRACTS

KEON, C.A., CLARKE, K., NEDELEC, J.F., ⁷Li NMR spectroscopy as a method to define mechanisms of transsarcolemmal sodium movements during ischemia and reperfusion, *Circulation* 84: II-17, 1991.

KEON, C.A., NEDELEC, J.F., ROKOSH, E., CLARKE, K. Lithium as a probe in the study of transsarcolemmal sodium movements in heart: ⁷Li and ³¹P NMR spectroscopic studies. SMRM 11th Annual Meeting, 1992.

KEON, C.A., NEDELEC, J.F., CLARKE, K. Characteristics of lithium relaxation in the perfused rat heart. SMRM 11th Annual Meeting, 1992.

PRESENTATIONS

1991

“Trans-sarcolemmal cation movements during ischemia and reperfusion: NMR spectroscopic studies.” Heart Research Lecture Series, Cardiovascular Research, The Rayne Institute, St. Thomas’ Hospital, London, December 16, 1991.